Experimental investigation on performance characteristics of A653 galvanized steel sheet using Fiber laser cutting process

A Dissertation submitted
in partial fulfillment of the requirements
for the degree of

Master of Engineering

in

Production Engineering

by

Gaurav Sharma
(801382007)

Under the Supervision of
Dr. V.K. Singla
Associate Professor

MECHANICAL ENGINEERING DEPARTMENT

THAPAR UNIVERSITY, PATIALA

July, 2015

CERTIFICATE

I hereby declare that the thesis entitled "**Experimental investigation on performance characteristics of A653 galvanized steel sheet using Fiber laser cutting process**" is an authentic record of my work carried out as requirements for the award of the degree of **Master of Engineering** in **Production Engineering** at **Thapar University, Patiala** under the supervision of **Dr. V.K. Singla**, Associate Professor, Mechanical Engineering Department, Thapar University, Patiala during July, 2013 to July, 2015. No part of the matter embodied in this report has been submitted to any other University or Institute for the award of any degree.

Date: 14/07/15

Gaurav

Gaurav Sharma
(801382007)

It is certified that the above statement made by the student is correct to the best of my/our knowledge and belief.

Dr. V.K. Singla
(Supervisor), Associate Professor
Mechanical Engineering Department
Thapar University, Patiala - 147004

Countersigned by

Dr. S.K. Mohapatra
Head, Mechanical Engineering Department
Thapar University, Patiala – 147004

Professor, S.S. Bhatia
Dean of Academic Affairs
Thapar University, Patiala – 147004

Acknowledgement

It gives me a great sense of pleasure to present the report of the thesis work undertaken during ME second year. I owe special debt of gratitude to **Dr. V.K. Singla, Associate Professor, Department of Mechanical Engineering** for his constant support and guidance throughout the course of our work. His sincerity, thoroughness and perseverance have been a constant source of inspiration for us. It is only his cognizant efforts that our endeavors have seen light of the day.

I also take the opportunity to acknowledge the contribution of **Dr. S.K. Mohapatra, Senior Professor and Head, Department of Mechanical Engineering** for his full support and assistance.

I also do not like to miss the opportunity to acknowledge the contribution of all faculty members of the department for their kind assistance and cooperation. Last but not the least, I would like to thanks my parents and friends for their encouragement and support during odd times and showing the right direction of path.

GAURAV SHARMA

(801382007)

Abstract

In laser beam cutting process the cut quality is most important. The quality of laser cut is determined by the kerf width and kerf deviation. Nowadays industries are demanding uniform kerf with minimum kerf width. The present work explores the modelling and optimization of laser beam cutting process parameters during fiber laser cutting of A653 Galvanized steel sheet for straight cut using different optimization techniques. The four input process parameters gas pressure, power, frequency and feed rate are investigated to check their effect on quality characteristics like kerf width (KW), kerf deviation (KD) and material removal rate (MRR) have been taken for the experimentation work. The multi-response optimization of process parameters has been done to improve geometrical accuracy by minimizing the kerf width and kerf deviation. Response surface methodology (RSM) technique was used to optimize the process parameters with considering the interactions. The Box–Behnken design had been utilized to plan the experiments, and response surface methodology was employed for developing the empirical models. The desirability function approach has been used for multi-response optimization. The predicted optimum result has been validated by performing the confirmation test. The confirmation result showed the percentage prediction error in kerf width, kerf deviation and MRR were 5.12 %, 5.88 % and 2.56 % respectively. Result shows the predicted model is adequate. Taguchi based fuzzy logic technique was used to optimize the process parameters assuming no interaction between the factors. The experiments were planned according to the Taguchi's experimental design L_{27} Orthogonal Array. The S/N ratios taken for the KW and KD is of the smaller-the-better type and MRR is of the higher the better type . The predicting fuzzy logic model is implemented on Fuzzy Logic Toolbox of MATLAB using Mamdani technique. The fuzzy logic theory has been applied to compute the fuzzy multi-response performance index (FMRPI). This performance index was further used for multi-objective optimization. The predicted optimum results have been validated by performing the confirmation tests. The confirmation tests showed the considerable reduction in kerf width, kerf deviation and increase in material removal rate. Scanning electron microscope and Energy dispersive spectroscopy has been done to analyses HAZ and recast layer formation for the selected laser machined samples. It has been concluded that average thickness value of HAZ is increased as increase in power and

frequency. The formation of recast layer decreases as gas pressure increases, the size of recast layer mainly depends on gas pressure.

Key words: Laser beam machining; Kerf width; Kerf deviation; RSM; Fuzzy logic; Multi-response optimization.

Contents

List of Figures

List of Tables

Nomenclature

β_O = Constant term
β_i = Coefficients of linear terms
β_{ii} = Coefficients of quadratic terms
β_{ij} = Coefficients of interaction terms
xi = Independent quantitative process variables
Y = Response variable
r = Number of experimental trails
y_i = Experimental value of quality characteristics for ith experimental run
μ_m = Total mean of FMRPI
μ_i = Mean of FMRPI at the optimal level
n = Number of control factors

Acronyms

LBM	≡	Laser Beam Machining
KW	≡	Kerf Width
KD	≡	Kerf Deviation
MRR	≡	Material Removal Rate
ANOVA	≡	Analysis of Variance
ANN	≡	Artificial Neural Network
FL	≡	Fuzzy logic
RSM	≡	Response Surface Methodology
HAZ	≡	Heat Affected Zone
S/N	≡	Signal to Noise
SEM	≡	Scanning Electron Microscope
EDS	≡	Energy Dispersive Spectroscopy
FMRPI	≡	Fuzzy multi response performance index

Chapter 1

Introduction

Due to the advancement in engineering material, design requirement, tight tolerance, micro-machining, complex size and shape of work material, the use of traditional machining processes become impossible. To tackle this kind of jobs the unconventional machining processes (UMPs) are used. Unconventional machining processes do not use conventional tool for machining. Today in industries many UMPs are being used like laser beam machining, plasma beam machining, abrasive jet machining, electrochemical machining, electron beam machining, ultrasonic machining, electro discharge machining, but all these processes have their own applications and limitations. [Dubey and Yadava, 2008a]

1.1 Laser beam machining

Laser stands for light amplification by stimulated emission of radiation. The underline working principle of laser was first put forward by Albert Einstein in 1917. The first industrial laser was developed in 1960 and has generally used for cutting, marking, welding, drilling, sintering and surface treatment [Dubey and Yadava, 2008a]. Laser cutting is most widely used LBM process. Laser cutting can be used for all advanced engineering materials such as composites, plastics, ceramics and reflected metals either conductive or non-conductive.

Laser is a coherent, convergent and monochromatic beam of electromagnetic radiation with wavelength varying from ultra-violet to infrared (0.1 μm to 70 μm). The rays of a laser beam are perfectly parallel and monochromatic, so that it can be focused to a very small diameter and produce a power density as high as $10^7 W/mm^2$ [Gosh and Mallik, 2012]. Laser can produce very low mW to extremely high (1-100 kW) focused power with precise spot size [Majumdar and Manna, 2013]. The main feature of laser cutting as it is a non-contact process, it does not involve any tool wear, vibration and mechanical cutting forces. LBM is the thermal energy based process. Laser beam machining capability mainly depends on optical and thermal properties irrespective of mechanical properties, which exhibit of high degree of hardness and brittleness [Pandey and Dubey, 2012; Dubey and Yadava, 2008a].

1.2 Principle of LBM

In thermal equilibrium state the number of atoms in lower energy level is much more than the number of atoms in higher energy level. The population of atoms at each energy level is depends upon the difference in energy and temperature. As the increase in energy the population at each energy level decreases. When an atom is absorbs a quantum of energy from external source (light source) the orbital electrons of an atom which is in lower energy state jumps to the higher energy state. Lately electron drop to it's original low energy level i.e. transition from higher energy level to lower energy level it emits absorb energy. Basic processes required to produce laser beam are spontaneous emission, stimulated emission and population inversion.

1.2.1 Spontaneous emission

At absolute zero temperature an atom is considered as in ground state. These electrons can be excited by absorbing energy from external source. The electrons jump to higher energy level from the lower energy level. At higher energy level the electrons are unstable. Excited atoms at higher energy level E_2 may spontaneously come back to lower energy level E_1 by releasing a photon as seen in Fig. 1.1. This process is called spontaneous emission.

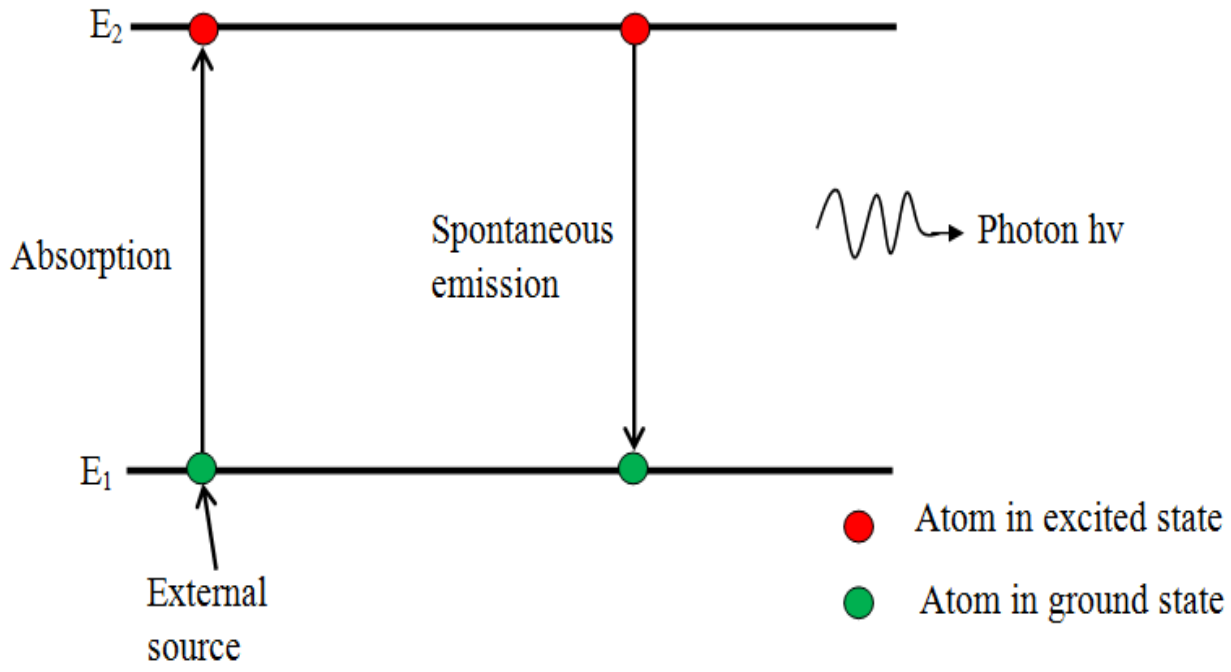

Figure 1.1: Spontaneous emission [Laser beam machining, W.1]

1.2.2 Stimulated emission

The process of absorption and spontaneous emission of photon cannot amplify the light. It requires to unstable the atom in higher energy state by passing a photon of frequency ω. At higher energy level electron stay for very small time and comes back to ground level immediately. The pump photon encourages the electron to decay at that point and provides the second photon of same frequency in phase with the first photon is shown in Fig.1.2. This process is called stimulated emission.

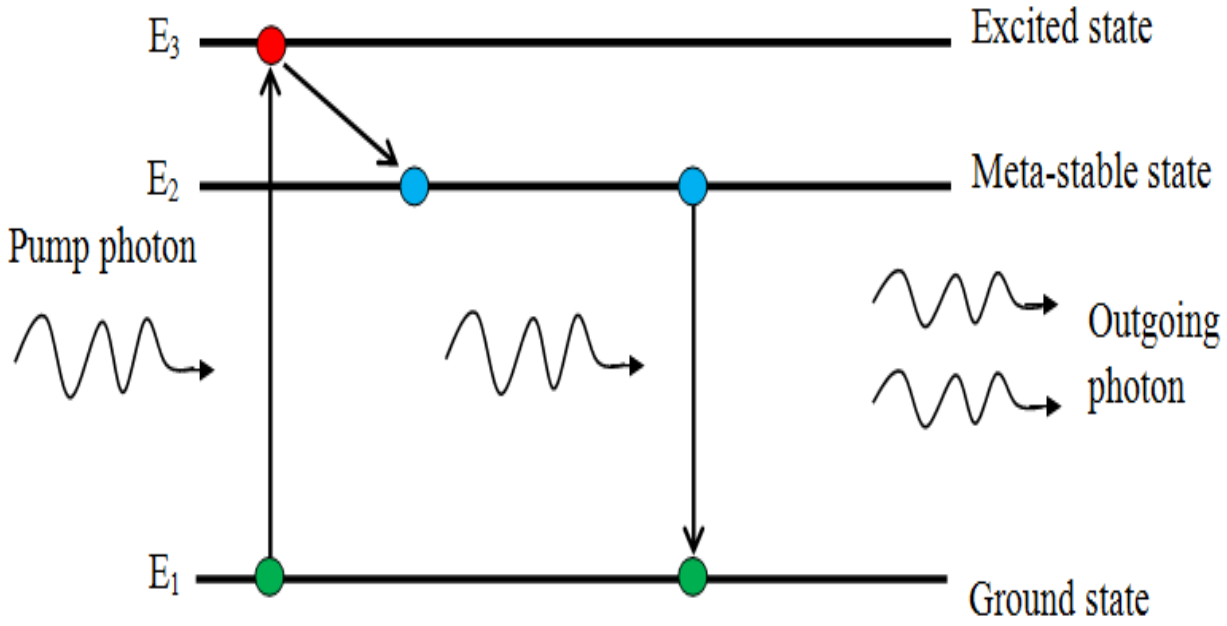

Figure 1.2: Stimulated emission

1.2.3 Population inversion

It requires the additional energy for pumping the more number of electrons at higher energy state than the lower energy state. The population of electrons increased in higher energy level increase the net intensity of system. This is called population inversion. This is not achieved by two energy states. In most of the lasers used three or four energy levels for population inversion. In three energy levels the electrons are jump to E_1 to E_3 by some pumping source. The electrons in higher energy level E_3 comes back to meta-stable state E_2 in very short time without release a photon (radiation less transition). The population of exited state atoms gathers in E_2 thus

population inversion is achieved between E_2 and E_1. Then electrons in meta-stable state E_2 decay to ground state E_1 by spontaneous emission.

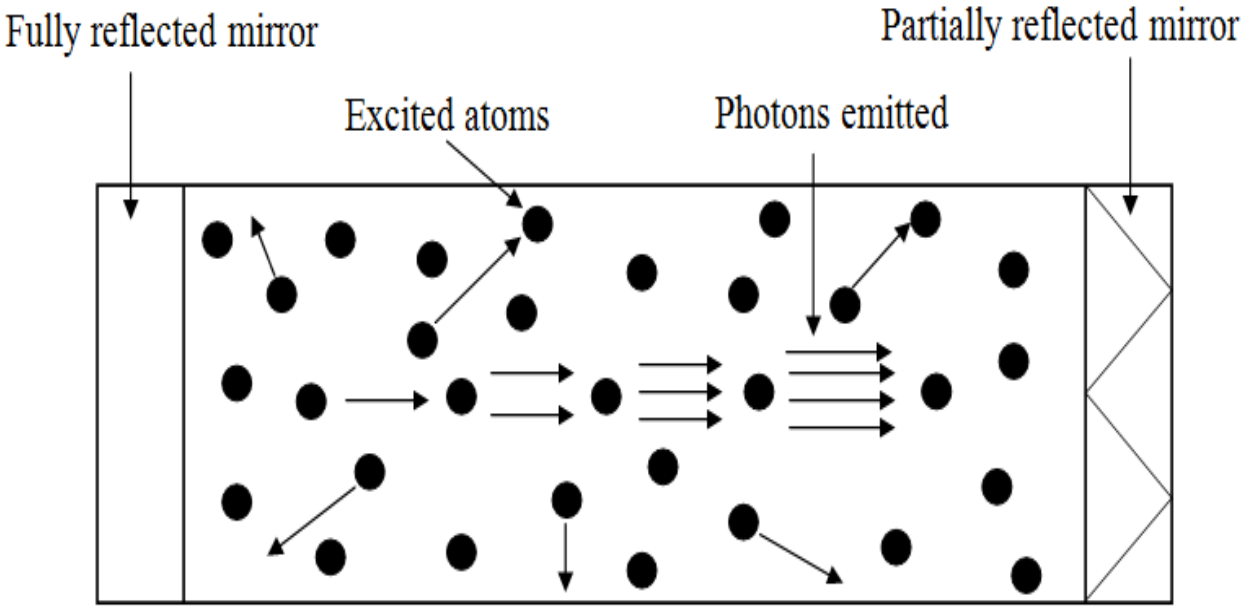

Figure 1.3: Lasing action [Laser beam machining, W.1]

When laser material placed in an optical cavity and exposed to light keep storing the energy that excites the element of material called lasing material. Population inversion takes place by exciting the element of material by pumping it with flash lamps. Lasing action occur due to stimulated emission is shown in Fig. 1.3. The energy emitted in the form of highly amplified light beam. This light beam is coherent, highly collimated and monochromatic is known as laser beam.

1.3 Laser cutting

The output of a high power laser beam is directed in a programmed manner towards the material by control unit. Mirrors have crucial role in production of laser and their application and is used to direct the beam from source to lens. Optical lens is responsible for focus the beam into the workpiece and focal length can be adjusted with the help of lens as per the application. The high energy density laser beam produces high amount of heat thus melts or vaporizes the material at focused zone. Assist gas is used to remove the molten material which doesn't get vaporized from the cutting region. Figure 1.4 shows the schematic of laser beam cutting process. The control unit helps to achieve the desired shape and profile of workpiece with the use of computer program.

Laser beam cutting is thermal process. It cut almost all material irrespective of its physical properties or hardness.

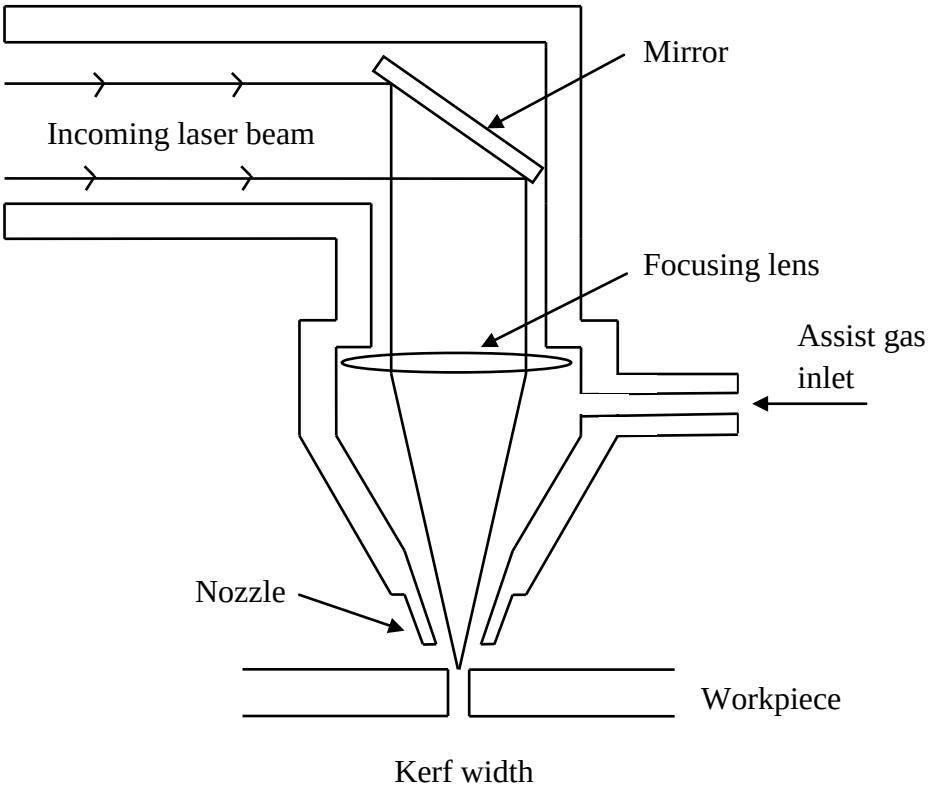

Figure 1.4: Schematic of laser beam cutting process [Dubey and Yadava, 2008a; Dubey and Yadava, 2008b]

1.4 Types of Lasers

1.4.1 Based on mode of operation

Lasers may be continuous wave mode or pulsed wave mode. In continuous mode the laser output power is constant over the time without any interruption it works. It is used for cutting generally straight profile. In pulsed mode the laser output power is interrupted. It is used for cutting thin material and complex geometry corners.

1.4.2 Based on lasing medium

Lasers are classified into solid lasers (ruby laser and Nd:YAG), liquid lasers (dye) and gas lasers (CO_2, He-Ne, Ar) [Dubey and Yadava, 2008a].

Solid lasers

In solid state laser the gain medium is such as crystals or glasses doped with rare earth elements such as neodymium, ytterbium and chromium are most commonly used. Most common solid state lasers are ruby laser, neodymium-doped yttrium aluminium garnet (Nd:YAG) and neodymium-doped glass (Nd:glass). In ruby laser xenon flash tube is located over the ruby rod and internal surface made highly reflecting for pumping operation [Gosh and Mallik, 2012]. The laser beam focused with help of lens system and focused beam interact with workpiece and remove material by melting or vaporization. Nd:YAG (neodymium-doped yttrium aluminium garnet) used as a lasing medium in Nd:YAG laser doped with neodymium and yttrium. Nd:YAG have wavelength of 1.06 μm. It is suitable for drilling small holes and also be used for engraving and etching.

Gas lasers

Gas is used as active gain medium for gas lasers. The most common gas lasers are CO_2, helium-neon laser and argon laser. The advantages of gas lasers are that it produces homogeneous laser medium, inexpensive and efficient and easy cooling. CO_2 is highly powerful and used in both continuous as well as pulsed mode. It has wavelength of 10.6 μm and pumping operation is achieved by electrical discharge. The main application of CO_2 laser in cutting and welding, it is capable of cutting 50 mm thick carbon sheet.

Fiber laser

In fiber laser the light is guided through single mode optical fiber and fiber allows light to be easily delivered to a movable focusing element. Fibers have high surface area to volume ratio which provides efficient cooling. In fiber laser active gain medium optical fiber doped with ytterbium and erbium ions. The excitation energy is provided by laser diodes. The wavelength of laser beam is in range 1.07 μm to 1.09 μm. It provides the high output power and high quality optical beam by eliminate the thermal distortion of optical path. The fiber laser is designed as double-clad fiber and the reflectors used are physically different from traditional lasers [Shah et al., 2014]. The fiber laser is useful because it is stable, produces high quality of beam with high power and provides efficient cooling.

1.5 Process parameters in laser beam machining

Large number of process parameters affects the laser machining process is shown in Fig. 1.5. Cause and effect diagram of laser beam machining shows the process parameters which affect the performance of LBM. In beam geometry the beam diameter is describes the how fine and accurate it cut on workpiece and beam power density shows the intensity of laser power that how deep and fast it cut on workpiece. According to the application requirement the type of laser and mode of operation is considered. For each application a specific laser is used to get the best results. Workpiece material type, composition, mechanical properties and metallurgical properties are required for laser beam machining.

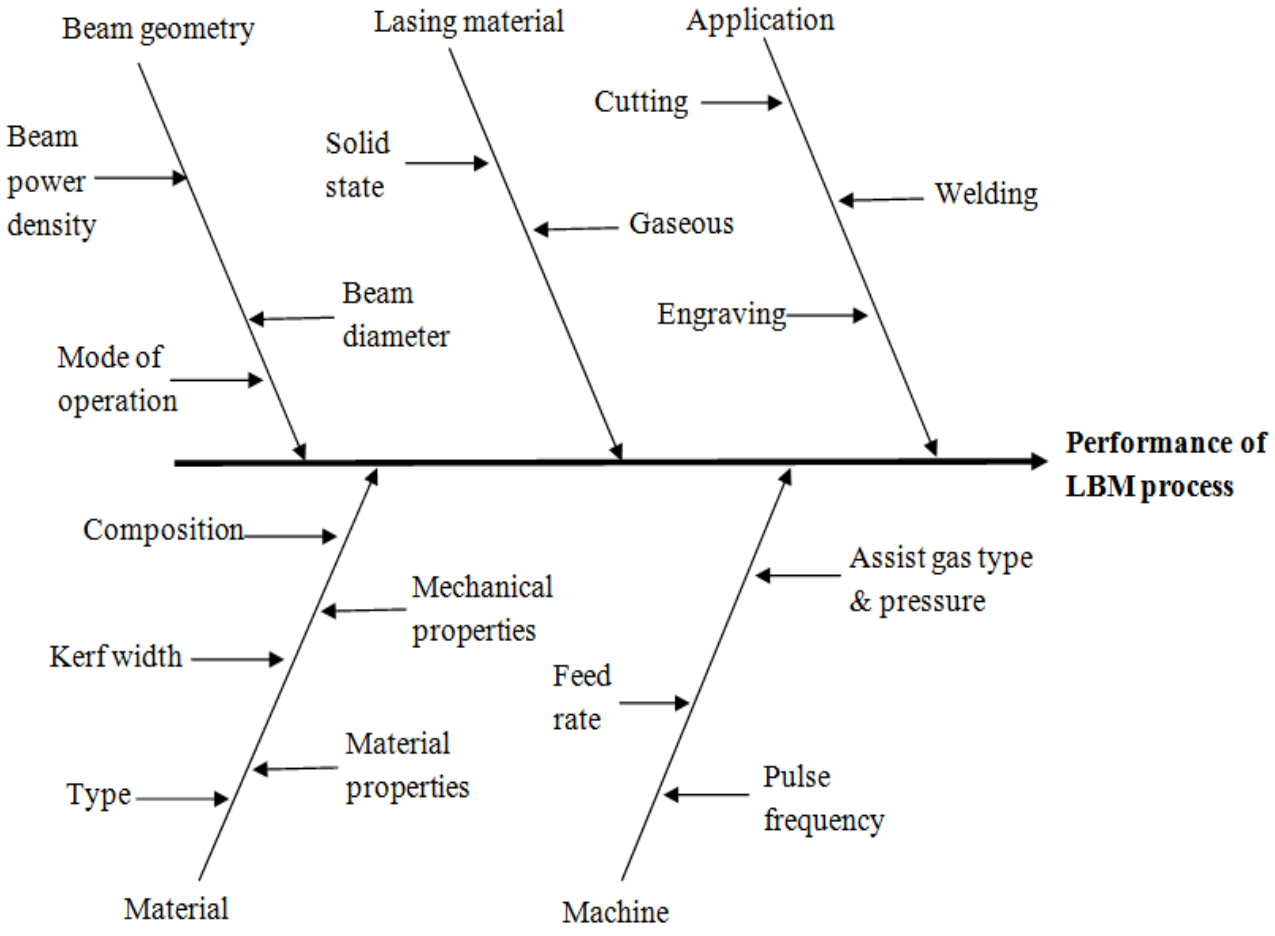

Figure 1.5: Cause and effect diagram of Laser beam machining

Literature review on laser beam cutting show the most common input process parameter which effects the process performance such as assist gas type and pressure, laser power, mode of

operation, feed, workpiece material thickness, type and composition [Dubey and Yadava, 2008a; Shah et al., 2014].

1.6 Quality characteristics of laser cutting process

The overall laser cut quality describes by following responses:

1) The kerf width, kerf deviation and kerf taper show the machined surface geometry.

2) Surface roughness and surface topography shows the surface quality of machined surface.

3) Heat affected zone (HAZ) and recast layer shows the metallurgical characteristics of machined surface.

4) Mechanical properties of machined surface describes by hardness and strength.

1.6.1 Kerf width

It is define as width of material that removed by cutting process. It represents the amount of material removed during process. To get the better quality cut the value of kerf width always required to be minimal. The nature of the kerf width is smaller the better type.

1.6.2 Kerf deviation

Kerf deviation shows the uniformity of the cut. It is the difference of maximum KW and minimum KW measured along the length of cut. It always desire to get uniform cut as the value of kerf deviation increases the uniformity of the cut decreases and cut quality get worse. The value of kerf deviation always required minimum.

1.6.3 Surface roughness

Surface roughness shows the irregularity and unevenness present in the laser cutting surface profile. Surface roughness always requires smaller the better. Surface roughness defines the surface quality of machined sample, it always required to be smaller the better. The most common profile roughness parameters are R_a and R_z. R_a shows the average roughness value of surface profile and R_z shows the average maximum height of the profile.

1.6.4 Heat affected zone

At the time of laser cutting process the excess amount of heat is transmit to the near cut edge. This excess amount of heat changes the metallurgical and physical properties of affected region of workpiece is known as heat affected zone.

1.6.5 Recast layer

Recast layer formed when molten material resolidified on work surface without ejected by assist gas. The molten material gets adhered to the workpiece lead to the formation of recast layer. It affects the mechanical properties and surface quality of work material.

1.6.6 Material removal rate

Material removal rate is defined as the amount of material removed per unit time. The nature of the material removal rate is larger the better type. MRR increases the production rate.

1.7 LBM Applications

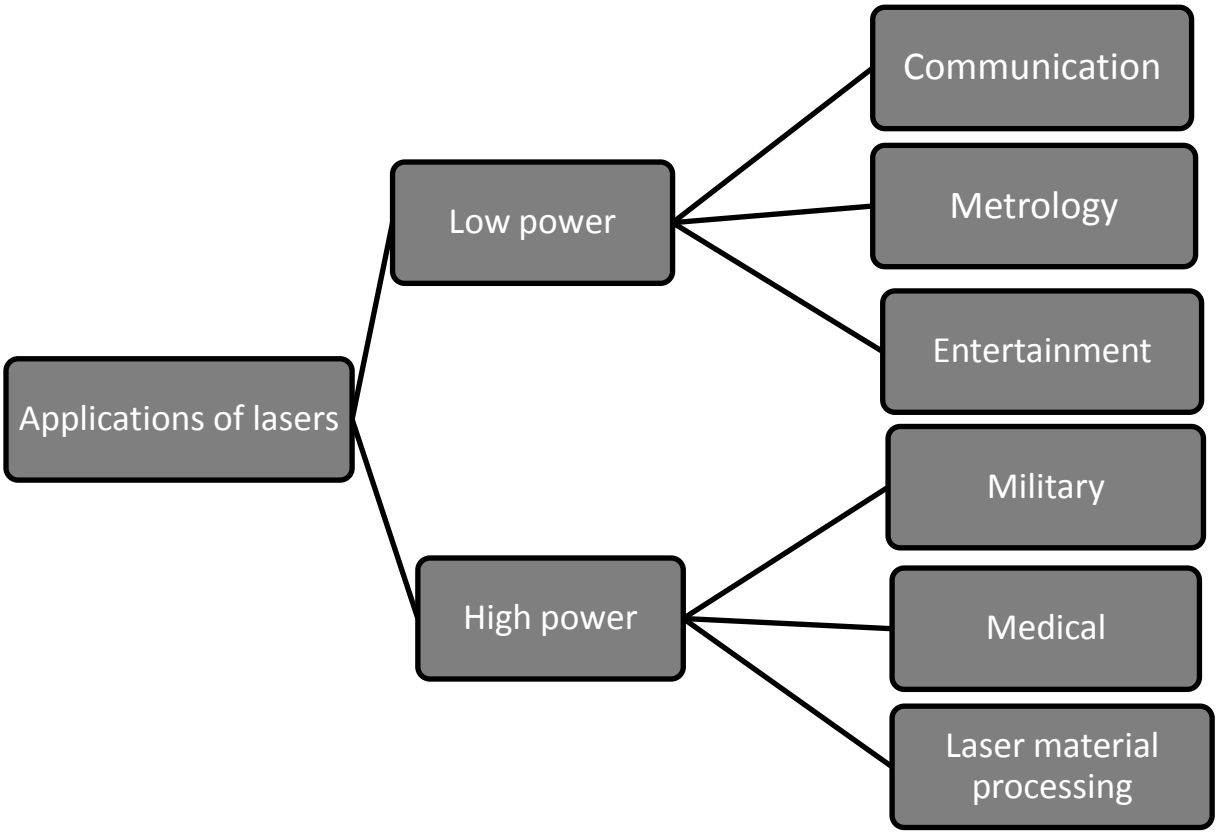

Figure 1.6: Applications of lasers [Majumdar and Manna, 2013]

Figure 1.6 shows the overview of application of laser in different fields. The following applications are given below:

- Titanium alloy sheet mainly cut by LBM process with high accuracy and precision and has wide applications in aerospace industry.
- Electronics and automotive industry have major application of LBM.
- For producing very accurate and small size holes up to 5 microns in metals, plastics and ceramics etc. This process used in aerospace industry for making cooling holes in turbine engine.
- LBM process widely used for fine and accurate drilling, welding and cutting of metallic and non-metallic materials.
- In medical field LBM process used for making micro-cavities in bone and teeth tissues [Dubey and Yadava, 2008a]
- Application of Laser emerges in the field of rapid prototyping processes like stereo-lithography and selective laser sintering (SLS).
- In the field of civil structure for cutting very hard materials like concrete, marble and stone.
- CNC laser cutting has been used in production of clothes.

1.8 Advantages of LBM process

- LBM process is capable to cut all materials with high accuracy and ease irrespective of its physical property or degree of hardness and brittleness.
- It can cut any desired shape and profile of workpiece with the use of computer numerical control program.
- No physical contact occur in LBM process, the contact is electromagnetic radiation so no forces are induced during machining and no need to provide support to workpiece.
- Fragile materials are easily cut by laser cutting.
- It can produce very small holes with large aspect ratio and holes can be accurately located by using optical laser system.
- Produce high quality cut no need of finishing operation required that make it to increase in production rate and quality.

- LBM gives very small HAZ as compare to other unconventional machining process. It makes LBM suitable for micromachining applications [Dubey and Yadava, 2008a]

1.9 Limitation of LBM process

- LBM process involve high initial capital investment and high operating cost
- LBM process cannot drill blind holes precisely the laser holes are tapered to some extent.
- Reflected laser light beam can lead to safety hazards.
- The formation of HAZ and recast layer may change the mechanical properties of work material
- Assist gas is required to remove the molten material which gets adhered to the workpiece and cannot be vaporized.

Chapter 2

Literature Review

2.1 Introduction

This chapter presents literature review based on previous research papers related to Laser beam machining process. The literature review shows the different kinds of modelling and optimization techniques used in laser beam machining process. The literature review shall be used to discuss the effect of different control parameters and different method of modelling and optimization on the quality characteristics of laser beam machining.

2.2 Literature Review of LBM process

Chang and kuo [2007] evaluate the value of surface roughness for aluminium oxide during laser-assisted turning process. Nd:YAG laser used for this purpose. The experimental plan was based on L_9 orthogonal array. Four input parameters rotational speed, depth of cut, feed and pulse frequency were considered. The experimental results were analysed by using Taguchi method. It was found that higher rotational speed provides good surface finish. Rotational speed was the most significant parameter which effect laser assisted machining performance. The results indicate that laser assisted machining provides better surface quality than conventional machining process.

Dubey and Yadava [2008b] developed a hybrid Taguchi method and response surface method (TMRSM) approach used for multi-optimization of laser beam cutting of thin sheet of high silicon-alloy sheet. A 200W pulsed Nd:Yag laser cutting system with CNC work table and oxygen was used as assist gas. The four input parameters were taken at three different levels assuming no interaction between factors cover the gas pressure, pulse width, pulse frequency, cutting speed and two output parameters kerf width (KW) and material removal rate (MRR). A standard L_9 OA was selected for experimental design. Analysis of variance (ANNOVA), F-ratio and p-test were carried out to test the mathematical models. The optimum value of KW and

MRR obtained from multi-optimization using taguchi method were 0.3733 mm and 124.1095 mg/min respectively while using the hybrid approach these values were 0.3267 mm and 169.1667 mg/min. It was found that the improvement in both the parameters with hybrid approach TMRSM, so hybrid approach gives the best results as compared to only taguchi method.

Dubey and Yadava [2008c] optimized the kerf quality during Nd:YAG laser beam cutting of aluminium alloy sheet of 0.9 mm thickness. In present research, two kerf qualities such as kerf width and kerf deviation (unevenness along the length) had been optimized by using Taguchi quality loss function. It was found that assist gas pressure and pulse frequency significantly affect kerf quality. It was observed that the considerable reduction in kerf width and kerf deviation achieved.

Dewangan et al. [2015] studied the investigation of various EDM process parameters like pulse current, pulse-on time, tool work time and tool lift time on various aspects of surface integrity like white layer thickness (WLT), surface crack density (SCD) and surface roughness (SR). A response surface methodology (RSM) based design of experiment had been considered for this purpose. The simultaneous optimization of multiple attributes achieved by using Fuzzy-TOPSIS based multi-criteria decision making (MCDM) approach. This technique was found adequate for simultaneous optimization of multiple attributes.

Ghosal and Manna [2013] optimized different parameters of ytterbium fiber laser using Response surface method. Experiments were performed on Al/Al_2O_3-MMC work-piece. Response surface methodology was used for experimental design. Different machining parameters were taken such as laser power, gas pressure, pulse width, modulation frequency, wait time and performance parameters metal removal rate and tapering phenomena has been considered. The developed mathematical models can directly used for evaluation of MRR & taper angle. It was reported that material removal rate increase with increase of N_2 gas pressure. It was found that the optimal parametric value for maximized MRR & minimized taper was 19.82 bar nitrogen gas pressure, 604.54 Hz modulation frequency, 473.12W laser power, 0.18 s wait time and 93.47% pulse width.

Kumar et al. [2013a] investigated the wire electric discharge machining process parameters and surface integrity. The Box-Behnken design technique was used for plan the experiments. Response surface methodology was employed for developing mathematical models. Six machining parameters and three responses were considered such as wire wear ratio, material removal rate and surface roughness for machining of pure titanium. Scanning electron microscope, energy-dispersive X-ray analysis and X-ray diffraction techniques were used to check the surface morphology. The migration of tool elements absorbed by XRD pattern analysis and different compound formation occur such as titanium dioxide, ilmenite and copper titanium dioxide. At higher spark frequency and peak current the wire rupturing occurred. Confirmatory experiments were conducted to validate the model. The percentage prediction error for WWR, MRR and surface roughness was 5.79 %, 6.95 % and 7.25 % respectively.

Madic et al. [2012] developed empirical model by using artificial neural network and experimental data collected. Taguchi's orthogonal array was implemented for experimental plan.CO_2 laser oxygen was used as assist gas, cutting of 2mm thick mild steel was studied to check the surface roughness. Surface roughness affects fatigue life, friction, wear and tear of parts. The main cutting parameters such as cutting speed (v), laser power (P) and assist gas pressure (p) were taken as input parameters. Taguchi's standard L_{25} orthogonal array was used. The 19 data was taken for mathematical model development and 6 data for model testing. The surface roughness was described by average surface roughness (R_a) and ten-point mean roughness (R_z). Thus, the effect of laser cutting parameters on the R_a and R_z can be studied using developed ANN models as shown in Fig. 2.1.

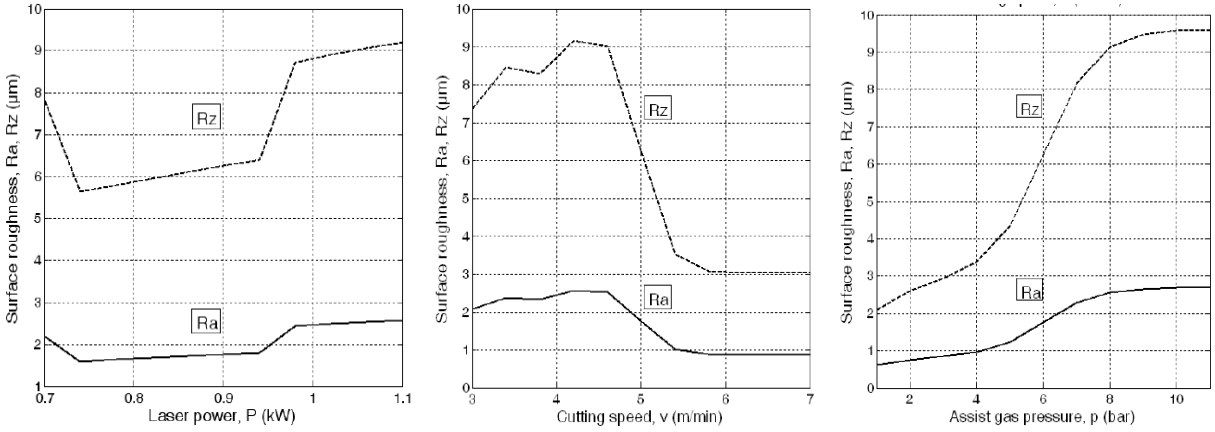

Figure 2.1: Effect of laser cutting parameters on *Ra* and *Rz* [Madic et al., 2012]

ANN model for R_a the average errors for training and testing data are 1.85 % and 7.73 %, respectively. In the case of ANN model for R_z the average errors for training and testing data are 2.19 % and 11.87 %, respectively. These results indicate that ANN predictions are in good agreement with the experimental results.

Madic et al. [2013] used the application of Taguchi method for optimization in surface roughness in CO_2 laser cutting of mild steel using the oxygen as assist gas purity of 99.95%. Three laser cutting parameters, cutting speed, laser power and assist gas pressure were considers. The experiment was planned according to the Taguchi's experimental design by using L_{25} OA. Two major tools used in Taguchi optimization methodology were orthogonal arrays (OA), and signal to noise (S/N) ratio. The S/N ratios give the optimal combination of the parameter levels, where the variance was minimum. Here smaller the better type S/N ratio was taken for surface roughness. It was noticed that the cutting speed should be kept at the highest level (7m/min), assist gas pressure at the lowest level (3 bar), while laser power should be kept at an intermediate level (0.9 kW) for obtaining minimal surface roughness. It was found that cutting speed and assist gas pressure were the most significant parameters affecting the surface roughness, whereas the effect of the laser power was very smaller.

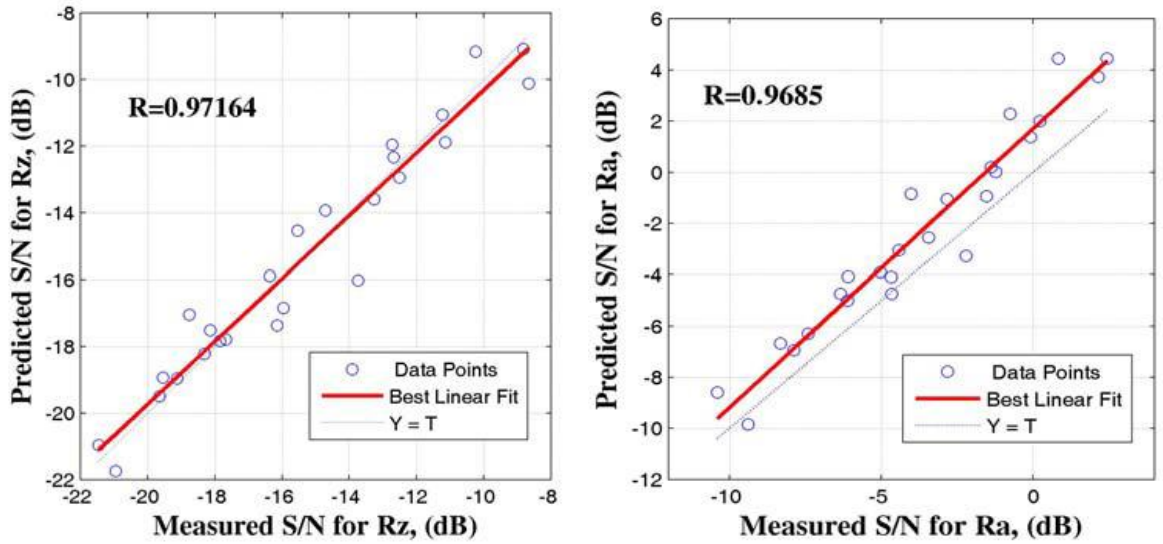

Figure 2.2: Comparison of measured and predicted values of S/N ratio for: (a) *Ra*, and (b) *Rz* [Madic et al., 2013]

Pandey and Dubey [2011] used the hybrid approach of Artificial Neural Network (ANN) and Fuzzy Logic (FL). Adaptive Neuro Fuzzy Inference System (ANFIS) was used to develop the Kerf width and Material removal rate (MRR) models. Thin steel sheet was used as material. These ANFIS models were developed by using "ANFIS EDIT" tool box of MATLAB. The data predicted by ANFIS models have been compared with the data obtained from RSM based models. ANFIS utilized the mathematical properties of ANNs in tuning rule-based fuzzy systems that approximate the way human's process information. Four input process parameters such as pulse frequency, pulse width, cutting speed and assist gas pressure were considered. The standard deviation for ANFIS models of KW and MRR was 0.0458 and 27.89 respectively.
Standard deviation for RSM based models of KW and MRR was 0.0584 and 29.35 respectively. For ANFIS models of KW and MRR, the root mean square error (RMSE) was 0.0137 & 4.19 where as for RSM models 0.08576 & 4.46 respectively. For ANFIS models of KW and MRR, the mean average percentage error (MAPE) was 0.9955 & 2.49 where as for RSM models 5.6245 & 6.92 respectively. The values of KW and MRR predicted by developed ANFIS based models were quite close to that of values obtained from the experiments data. The comparison of these models with RSM based models show that kerf width and material removal rate values predicted by ANFIS based models were more reliable as compared to RSM based models.

Pandey and Dubey [2012] studied a hybrid approach, Taguchi based fuzzy logic optimization of multiple parameters which affect the geometric accuracy of laser cutting of duralumin sheet. The L_{27} OA based experiments were performed on Duralumin sheet with 200W pulsed Nd:Yag laser cutting system with CNC work table and oxygen was used as assist gas. The pilot experimentation was carried out to decide the range of the different control factors. Four input parameters were vary at three level that cover the gas pressure, pulse width, pulse frequency, cutting speed and three output parameters top kerf width(KW), top kerf deviation(KD_t) and bottom kerf deviation(KD_b). The fuzzy logic was applied to convert the S/N ratios of different quality characteristics obtained by taguchi methodology into a single fuzzy multi-response performance index (FMPI). The performance index was further used for multi-optimization. It was found that the optimum parameter values for gas pressure 11 kg/cm^2, pulse width 1.8 ms, pulse frequency 6 Hz, cutting speed 25 mm/min. The predicted optimum results have been verified by confirmation tests that shows almost negligible error of 1.65%. It was found that the

effect of oxygen gas pressure is the most significant factor followed by pulse frequency in laser cutting of highly reflective and thermally conductive material like duralumin. The confirmation test shows reasonable reduction in kerf deviations at top and bottom sides. Geometric accuracy of laser cutting of duralumin sheet improves by minimizing the kerf width and kerf deviation at top and bottom sides as shown in Fig. 2.3 and Fig. 2.4.

Figure 2.3: Scanned photographs of laser cuts at initial setting [Pandey and Dubey, 2012]

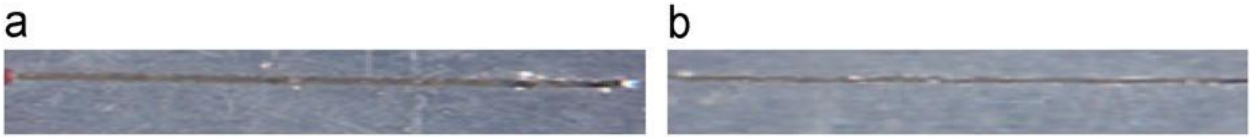

Figure 2.4: Scanned photographs of laser cuts at optimal setting [Pandey and Dubey, 2012]

Pandey and Dubey [2013] developed a fuzzy expert system for prediction of the laser cutting process behaviour of Ti alloy (Ti-6Al-4 V) sheet. A hybrid approach of neural network and fuzzy logic theory has been applied to develop the fuzzy expert system to predict the kerf widths and kerf deviation. The experiment was planned according to the Taguchi's experimental design L_{27} OA. Nitrogen used as assist gas, Ti-sheet of thickness 1.4 mm was used. Chemical Composition of Titanium Alloy sheet (Grade-5) (Al-6.22%, Fe-0.187%, Sn-0.56%, V-3.35%, Ti-89.6%). An exhaustive pilot experimentation was performed in order to decide the range of each control factor. The four process parameters such as assist gas pressure, pulse width or pulse duration, pulse frequency and cutting speed were considered and output responses were top kerf width (TKW), bottom kerf width (BKW) and bottom kerf deviation along the length of cut (KD). In pulsed mode Nd:Yag laser cutting, variation of peak power mainly governed by pulse width and pulse frequency, hence pulse width and pulse frequency have been found as the significant process parameter for the top as well as the bottom kerf width. The developed fuzzy expert system had been found adequate for prediction of the kerf qualities with negligible average prediction errors of 1.09%, 1.67% and 2.29% for top kerf width, bottom kerf width and kerf deviation respectively. The increase in pulse frequency significantly increases the kerf width due to increases in extent of spot overlap. The higher gas pressure results in lesser deviation in kerf.

Pawar and Rayate [2014] have presented the multi-objective optimization of laser beam machining process parameters. Most researchers had been used statistical methods such as Response surface method, Taguchi, Grey relation analysis, Principal component analysis etc. for multi-objective optimization, and these methods are based on weight approach and gives single optimum solution. The experiments were performed on CO_2 laser machine to cur 3 mm plate of stainless steel AISI 321. In present research, they use posteriori approach known as Non-dominated sorting genetic algorithm (NSGA). This approach provides the appropriate set of optimum solutions as per the requirement.

Phipon and Pradhan [2012] used Genetic Algorithm (GA) optimization technique to optimize the control parameters. The process control parameters were such as Oxygen pressure, pulse width, pulse frequency and cutting speed and the desired responses kerf taper and surface roughness respectively. Pulsed Nd:Yag laser used for cutting Al-alloy sheet for straight profile was performed. The Response Surface Methodology (RSM) was used to develop the mathematical model correlating the desired responses and the control parameters. RSM technique employed to design experiments with a reduced number of experimental runs to achieve optimum responses. MATLAB software was used to solve GA. GA provided minimum kerf taper was 0.14695 which was 0.313° less in magnitude than experimentally measured value. Similarly, using GA the minimum surface roughness predicted at optimal parameter setting was 1.2625μm which was 0.3375μm better in value compared to the experimental measured value. The percentage prediction error for kerf taper and surface roughness was 5.5% and 4.27 % respectively. GA provides a cost effective soft computing technique for optimizing machining operations.

Shabgard et al. [2013] used the fuzzy system for the selection of the electrical discharge machining (EDM) and US/EDM parameters and observations indicate that the fuzzy modelling results of EDM and US/EDM were in good agreement with experimental findings demonstrating approximately 90% predictions was achieved. So this shows that Fuzzy modelling technique could be an economical and successful method for modelling and optimization.

Shah et al. [2014] presented the review article on optimization of input parameters which affects the surface roughness during laser cutting. In this article the main objective was to find the most common process parameters and quality characteristics. It was found that laser power, cutting speed and gas pressure were the most common process parameters which affect the cut quality. The cut quality mainly depends on surface roughness, kerf width, kerf deviation and heat affected zone.

Sharma and Yadava [2012] developed two different hybrid approaches. One was used for modelling comprising of Taguchi methodology (TM) & Response Surface Methodology (RSM) was known as TMRSM. The second hybrid approach was used for multi-objective optimization known as TMGRA, comprising of TM & Grey relation analysis (GRA). The present research investigated the modelling and optimization of cut quality. The experiments were performed by pulsed Nd:YAG laser on thin Al-alloy sheet for straight profile. The four process parameters and two output parameters such as average kerf taper (Ta) and average surface roughness (Ra) were considered. The second order response surface model for R_a & T_a had been found adequate. The TMGRA approach reduces the T_a by 30.44 % and R_a by 6.25 %. The results showed that the TMGRA approach was effective tool for multi- objective optimization.

Sivarao et al. [2009] studied the graphical user interface (GUI) based Adaptive network fuzzy inference system (ANFIS) modelling approach in laser processing. Developed an ANFIS-LASER-GUI by using MATLAB to model and control the input parameters of a CO_2 laser cutting machine. Manganese-Molybdenum pressure vessel plate of thickness 5.0 mm was used as material. Total 128 experiments were conducted based on the DOE matrix. Seven input parameters namely; power, speed, pressure, focal distance, standoff distance, frequency, duty cycle with their respective two responses; surface roughness and kerf width were used. ANFIS-LASER-GUI generated output excellently correlates with the observed values performing prediction error below 9.0 percent. It was found that the MATLAB based Graphical User Interface (GUI) has been successfully developed and tested for its ability in modelling of laser processing by Adaptive network fuzzy inference system.

Syn et al. [2011] developed a mamdani type fuzzy expert system to prediction of laser cutting quality. The three input parameters were used such as power, cutting speed, gas pressure to predict the output surface roughness and dross inclusion. The CO_2 laser cutting process on material Incoloy alloy 800 with thickness 1.00 mm. The entire fuzzy logic model was implemented on FL Toolbox of Matlab. The both input and output fuzzied by Gaussian membership function and deffuzification was carried out by centroid method. It shows that the results predicted from FL model compared to experimental results were found to be satisfactory in terms of RMSE, R^2 and MAPE.

2.3 Summary of Literature

- Several authors have reported on the improvement in surface quality by using hybrid approach of optimization. The quality characteristics have been reported to show improvements with optimizing cutting speed, pulse width, pulse frequency and assist gas pressure [Pandey and Dubey, 2012; Dubey and Yadava, 2008a; Pandey and Dubey, 2013; Pandey and Dubey, 2011; Phipon and Pradhan,2012].
- Some authors have compared hybrid approach with taguchi method and Response Surface Methodology (RSM). It have been found that hybrid approach gives the best results as compared to only taguchi method and RSM [Dubey and Yadava, 2008b; Pandey and Dubey, 2011].
- The quality of laser cut is mainly depends on kerf width, kerf deviation and kerf taper [Dubey and Yadava, 2008c].
- Some authors have used artificial intelligence techniques for modelling and optimization of laser beam machining process [Syn et al., 2011; Sivarao et al., 2009; Pandey and Dubey, 2011].
- Some authors have reported on the Multi-objective optimization improve overall quality of product [Pandey and Dubey, 2011; Dubey and Yadava, 2008b; Ghosal and Manna, 2013].

2.4 Gaps Identified in the Literature Review

- Different control parameters mainly (cutting speed, pulse width, pulse frequency and assist gas pressure) have been studied by different researchers to improve the surface quality. Although, some other undesired factors which affect the performance variations such as (assist gas type, beam spot diameter, thermal conductivity and reflectivity of workpiece, focal distance, standoff distance) still need to be considered to increase the surface quality.
- Very few researchers concentrated on modelling and optimization of laser beam cutting through AI based techniques such as artificial neural network (ANN) and fuzzy logic (FL).
- Regression analysis is not useful for describing the non-linear complex relationship between process parameters and performance characteristics. AI based techniques are the alternative to provide adequate model.
- There should be limited work is done on other geometric profile like circular, curved and zigzag during LBM.
- Very limited literature has been reported on multi-objective optimization of LBM process to achieve improved quality characteristics.

Chapter 3

Experimental Methodology and Design

3.1 Introduction

This chapter contains the design study of our proposed work. It will include the basic information, research methodology, material, equipments and instruments required for laser cutting machined surface.

3.2 Material

A653 Galvanized steel sheet of thickness 0.5 mm was used for the experiments. The Galvanized steel sheet is basically carbon steel sheet coated with zinc on both sides. It is easy to fabricate and widely used for the applications where corrosion resistance is needed without the cost of stainless steel. The chemical composition of work material is shown in Table 3.1.

Table 3.1: Chemical composition of A653 galvanized steel sheet

Fe	C	Mn	P	S	Cr	Ni	Al	Cu	Ti	W
97.7	0.065	0.407	0.15	0.10	0.055	0.128	0.302	0.029	0.022	0.638

3.2.1 Applications

- The galvanized steel sheet used in electrical boxes, automotive parts, roofing, playground equipment, air conditioning system and protective railings.
- Steel water tank used for water storage and for fire protection purpose.
- Used in telecommunication towers and also used in building and construction purpose [Galvaco Industries, W.2]
- The galvanized steel sheet has long life and required less maintenance. In most rural environment the coating on structure member remains for 40-50 years.
- Economical and galvanizing cost is lower than other protective coating process.

- Galvanizing coating is toughest coating provides resistance to mechanical damage and no crack formation.

3.3 Equipments and Facilities

3.3.1 Fiber laser beam machine

The experiments were performed on 100 W Fiber laser beam machine (PATRIOT 100, Scantech Laser Pvt. Ltd.) 1ft × 1ft CNC work table fully integrated with hardware and software is shown in Fig. 3.1 (a) and Fig. 3.1 (b) shows the machine control unit of LBM. It is a continuous mode laser beam machine. The parameters kept constant during machining are thickness of material 0.5 mm, work material, assist gas type Oxygen, diameter nozzle 1 mm and distance between workpiece and nozzle tip (stand-off distance) was maintained at 2 mm.

(a) (b)

Figure 3.1: Experimental set up of Fiber laser machine (a) Fiber laser beam machine (PATRIOT 100, Scantech) [Machining Lab, Thapar University], (b) machine control unit of LBM

3.3.2 Measuring Equipments

Profile projector, weighing machine and spectrometer are used as measuring equipment in experimental study. The details of test equipments are given below as:

Profile projector

A Profile projector is an optical device utilized for measuring. The profile projector magnifies the surface features of sample and allow to measure it's dimensions. The main application of profile projector is in quality assurance department. The Nikon profile projector (Model V-10A) with 10 × magnification is available in Metrology Lab of Thapar University, Patiala is shown in Fig. 3.2. The voltage requirement is 220-240 V and current requirement is 0.6 A. The least count is 0.001 mm.

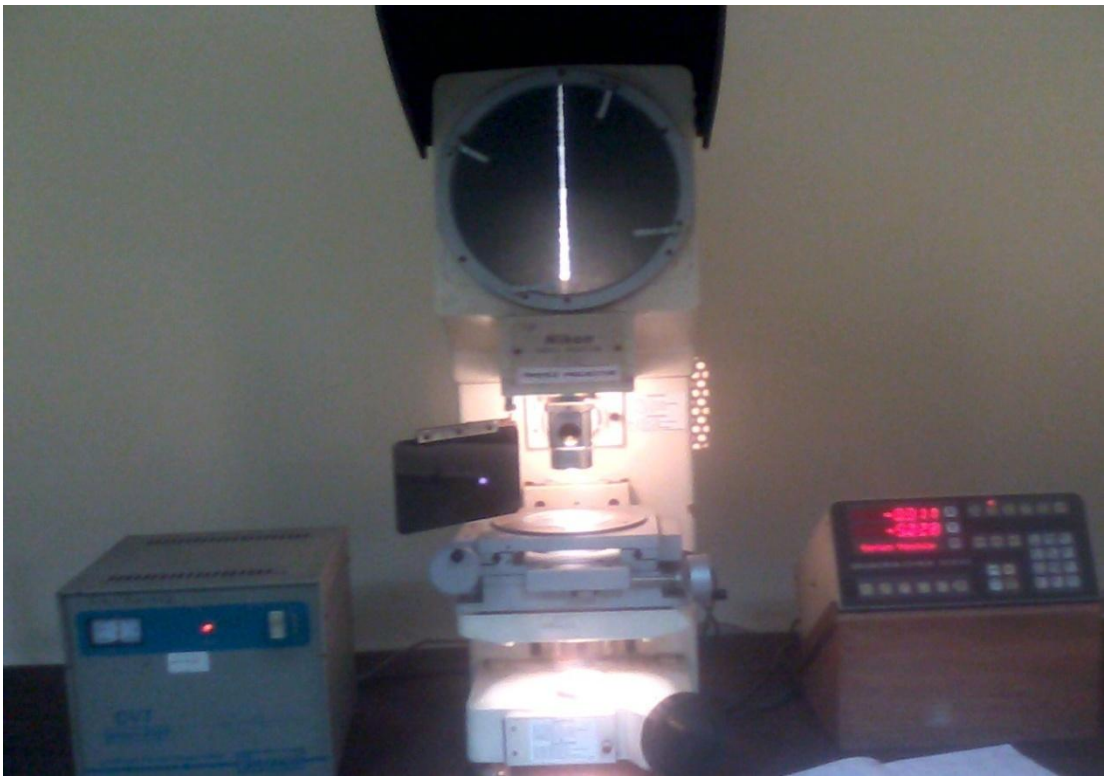

Figure 3.2: Profile projector [Metrology lab, Thapar University]

Weighing balance

The analytical Weighing balance is used to measure the weight difference of work piece before and after the laser cutting of sample using CAS Electronics balance (CAY 220) is shown in Fig. 3.3. The machine has least count of 0.1 mg and maximum capacity of 220 gm.

Figure 3.3: Analytical Weighing balance (CAY 220)

Optical Emission Spectrometer

The chemical composition of work piece material was measured using optical emission Spectrometer Foundry Master (Model DV-6) available at Thapar University, Patiala. Figure 3.4 shows the optical emission spectrometer. Argon gas is used for composition measurement process. The spark formed between the sample and electrode causes the electrons in the sample to emit light which is further used for spectral pattern. By measuring the peaks in this spectrum, it can produce material composition. An accuracy of 0.0001 % is achieved in this equipment.

Figure 3.4: Optical emission spectrometer [MED, Thapar University]

3.4 Pilot study

The pilot experiments were performed on 100 W Fiber laser beam machine (PATRIOT 100, Scantech Laser Pvt. Ltd.) 1ft × 1ft CNC work table fully integrated with hardware and software and peripherals. The process parameters for the experiments were decided on the basis of literature survey and pilot experiments conducted using one factor at a time approach (OFTA). Table 3.2 shows the following parameters kept constant during the experiments.

Table 3.2: Constant parameters during the experiments

Sr. No.	Parameters	Value
1	Stand-off distance	2 mm
2	Nozzle diameter	1 mm
3	Gas type	Oxygen
4	Material	A653 Galvanized steel sheet
5	Nozzle type	Conical

3.4.1 NC Program

The NC program code utilized during the experimentation work is shown below. The work sample cut in the form of square having dimensions 40mm (length), 40mm (width) and 0.5mm (thickness) for laser cutting process. Figure 3.5 shows the work-path and job profile during laser beam cutting process.

```
G54 G0 X0 Y0
G90
G01 X0 Y0 F1000
N110 G01 X5 Y20
N120 L2004
N130 G01 X35 Y20
N140 M11
N150 M13
N160 G01 X20 Y40
N170 L2005
N180 G01 X0 Y40
N190 G01 X0 Y0
N200 G01 X40 Y0
N210 G01 X40 Y40
N220 G01 X20.02 Y40
N230 M11
N240 M13
N250 M30
```

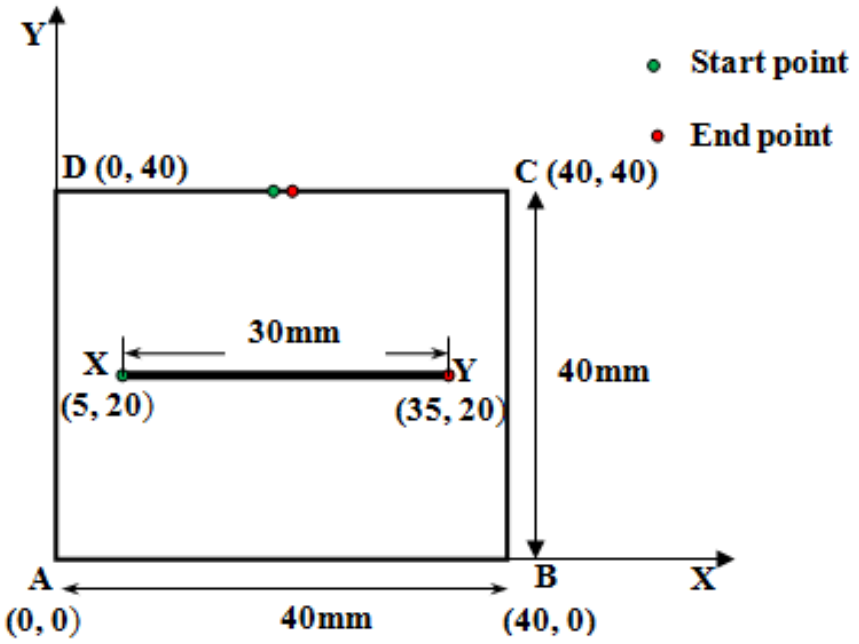

Figure 3.5: Work-path and job profile during machining

3.4.2 Results of Pilot experimentation

A straight cut of length 30 mm was made for each experiment as shown in Fig 3.5. The process parameters for the experiments were decided on the basis of literature survey and pilot experiments conducted using one factor at a time approach (OFTA).

Influence of different parameters on performance characteristics

The feed was varied from 100 to 600 mm/min in 4 steps as shown in Table 3.3. The other parameters like power, frequency and gas pressure kept constant and their values were given as 100 W, 100 Hz and 10 kgf/cm^2 respectively.

Table 3.3: OFTA Performance measure for Feed

Sr. No.	Feed (mm/min)	Kerf width (mm)	Kerf deviation (mm)
1	100	0.502	0.484
2	200	0.438	0.420
3	400	0.388	0.365
4	600	0.342	0.322

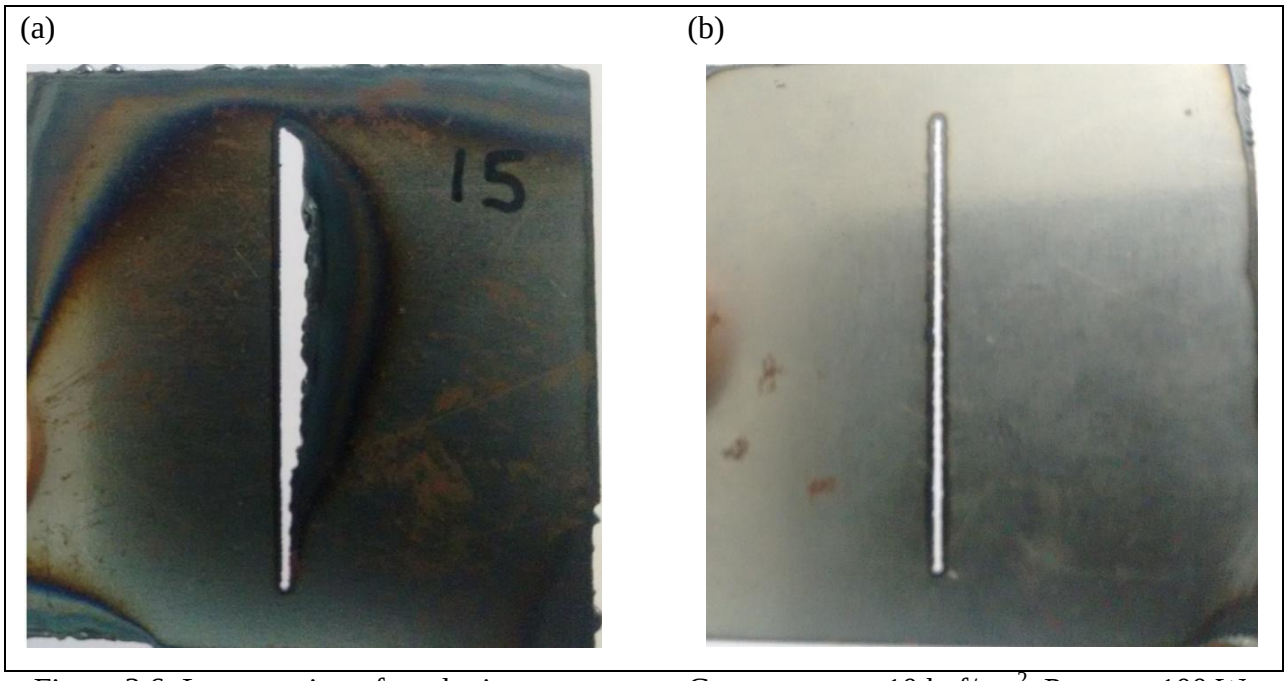

Figure 3.6: Laser cutting of work piece at constant Gas pressure = 10 kgf/cm^2, Power = 100 W, Frequency = 100 Hz and (a) when Feed = 100 mm/min (b) Feed = 600 mm/min.

It was observed that during low feed rate at 100 mm/min the value of kerf width was obtained much higher as shown in Fig. 3.6 (a). As the feed increases from 100 to 600 mm/min the value of kerf width start decreases. When the feed was less than 200 mm/min, it was observed that more material was burned which resulted in an increase in the kerf width and heat affected zone. To prevent these problem feed should be kept above 150 mm/min. Figure 3.6 (b) shows the laser machined workpiece at feed 600 mm/min resulted in decrease in kerf width and heat affected zone.

The gas pressure was varied from 4 to 12 kgf/cm^2 in 5 steps as shown in Table 3.4. The other parameters like power, frequency and feed kept constant and their values were given as 100 W, 100 Hz and 500 mm/min respectively.

Table 3.4: OFTA Performance measure for Gas pressure

Sr. No.	Gas pressure (kgf/cm^2)	Kerf width (mm)	Kerf deviation (mm)
1	4	0.498	0.450
2	6	0.436	0.400
3	8	0.384	0.350
4	10	0.274	0.375
5	12	0.312	0.420

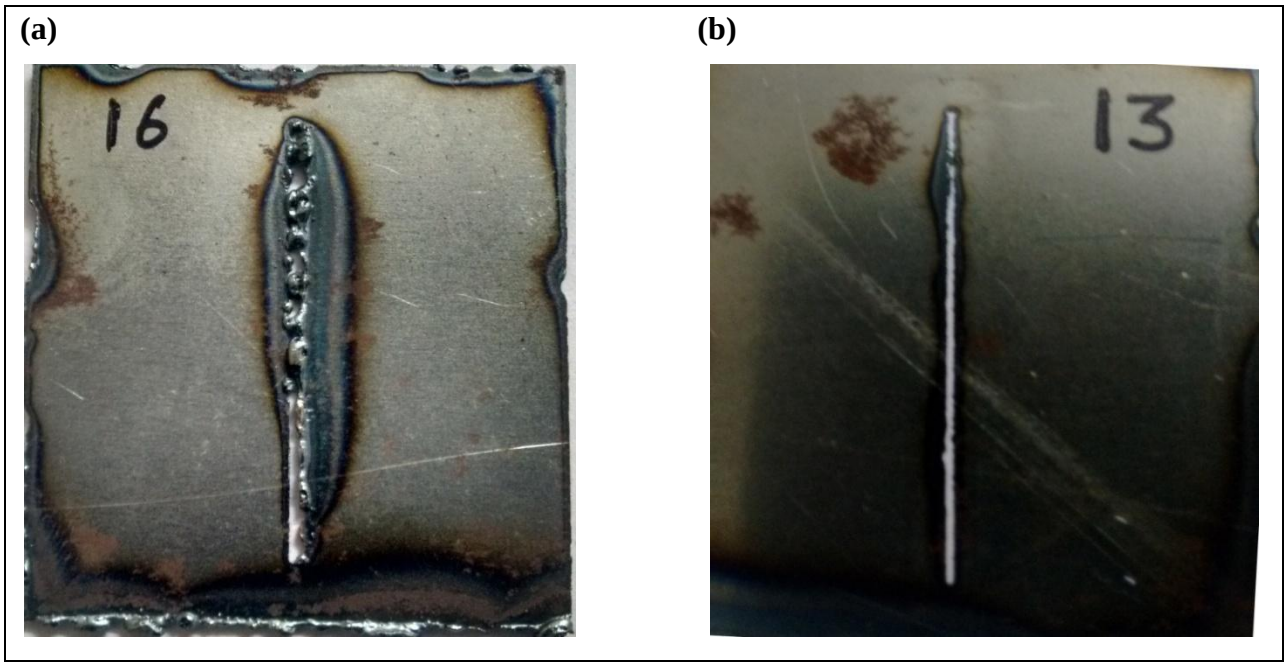

Figure 3.7: Laser cutting of work piece at constant Power = 100 W, Frequency = 100 Hz, Feed = 500 mm/min and (a) when Gas pressure = 4 kgf/cm^2 (b) Gas pressure = 12 kgf/cm^2

Low gas pressure leads to results in excessive burning, which degrades the edge quality and increase the kerf width and kerf deviation as shown in Fig. 3.7 (a). It was observed that as gas pressure increases from 4 to 12 kgf/cm^2 the formation of recast layer decreases. It occurred because as gas pressure increases more molten material blows away from the cutting zone so very less material left to resolidified to form recast layer. Figure 3.7 (b) shows the laser machined workpiece at gas pressure 12 kgf/cm^2 resulted in decrease in kerf width and recast layer.

3.4.3 Selection of Factors and their levels

The process parameters and their levels for the main experiments were decided on the basis of pilot study, using one-factor-at-a-time approach. Assist gas pressure, laser power, frequency and feed rate were selected as input process parameters (controllable factors). The output parameters selected for the analysis were Kerf width (KW), Kerf deviation (KD) and Material removal rate (MRR), which affect the quality of process (also known as quality characteristics). In this work, three levels of each control factor were selected. The control factors and their levels are shown in Table 3.5

Table 3.5: Control factors and their levels

Sr. No.	Factors	Symbol	Level 1	Level 2	Level 3	Unit
1	Gas pressure	A	6	8	10	Kgf/cm^2
2	Power	B	80	90	100	W
3	Frequency	C	50	70	90	Hz
4	Feed	D	150	300	450	mm/min

3.5 Measurement of Responses

In the current study, surface quality was characterized by machined surface Kerf width and Kerf deviation. The output parameters selected for the analysis were Kerf width (KW), Kerf deviation (KD) and Material removal rate (MRR).

3.5.1 Kerf Width

The width of laser cut is known as kerf width. It represents the amount of material removed during process. The value of kerf width always required to be minimal for better cut quality. For each experiment a straight cut of 30 mm was cut. Kerf width was measured at five different places for each cut along the length of cut. The average value of five measurements was taken as kerf width for each cut. Nikon Profile Projector (Model V-10A) with 10× magnification was used to measure the kerf width.

3.5.2 Kerf Deviation

Kerf deviation shows the uniformity of the cut along the length. The value of kerf deviation always required minimum to get the uniform cut. It is the difference of maximum KW and minimum KW measured along the length of cut.

The Kerf deviation (mm) was calculated as:

Kerf deviation = (Maximum kerf width-Minimum kerf width)

3.5.3 Material removal rate

The amount of material removed per unit time. The loss of the mass of work piece during laser cutting is measured by using CAS Electronics balance (CAY 220). The MRR (mg/min) was calculated as: MRR= (Loss of mass during each cut × cutting speed) / length of cut

3.5.4 Heat affected zone

At the time of laser cutting process the excess amount of heat is transmit to the near cut edge. This excess amount of heat changes the metallurgical and physical properties of affected region of workpiece is known as heat affected zone. The scanning electron microscope is used to measure the thickness of heat affected zone.

3.5.5 Recast layer

Recast layer formed when molten material resolidified on work surface without ejected by assist gas. The molten material gets adhered to the workpiece lead to the formation of recast layer. It affects the mechanical properties and surface quality of work material. The formation of recast layer can be easily seen from scanning electron microscope.

3.6 Modelling and Optimization

Modelling is the scientific way to study the system behaviour. Optimization is a mathematical procedure for determining optimal parameters and optimal allocation of scarce resources. A mathematical model of a system is the relationship between input and output parameters in terms of mathematical equations. The relationship between input and output parameters in terms of mathematical equations is provided by mathematical model. The models can classify in three categories:-

i. Experimental model
ii. Analytical model
iii. Artificial intelligence based model

3.6.1 Experimental methods

- Experiments in Response surface methodology (RSM) are performed using Box–Behnken design (BBD) matrix and other method like central composite design (CCD) to develop a second order response model. [Dubey and Yadava, 2008a]

- Taguchi methodology plan the experiments in such a way to nullify the effect of uncontrollable factors (noise) in order to make the process robust which is insensitive to noise factors.

3.6.2 Analytical methods

- Analytical models are the mathematical models based on basic laws and principles mainly are exact solution based model, numerical solution based model, and stochastic solution based model. Finite difference method (FDM), Finite element method FEM), Boundary element methods (BEM) are widely used in engineering sciences.

3.6.3 Artificial intelligence methods

- Artificial intelligence based techniques such as artificial neural network (ANN), Fuzzy logic (FL) and Genetic algorithm. Model developed based on FL deals with linguistic variables rather than operating on crisp values. The structure and function of ANN are similar to the way biological nervous systems work such as brain.

3.7 Response surface methodology

Response surface methodology provides relationships between several input variables and one or more response variables. In RSM, the experiments are performed by using Box–Behnken design (BBD) is used for planning and executing the subsequent main experimentation, as shown in Table 3.6. Response surface methodology (RSM) is a collection of statistical and mathematical techniques that are useful for provide a relationship between the input process parameters and output performance based on experimental results by employing regression analysis [Kumar et al., 2013a]. Finally, the analysis was done to study the main effects and their interactions to explore the quadratic effects of the influence of parameters on the performances. In general, a second-order regression model is developed because first-order models often give lack-of-fit.

Table 3.6: RSM Experimental design

Trail no	Gas pressure	Power	Frequency	Feed
1	8	90	90	150
2	6	100	70	300
3	8	100	70	150
4	8	100	90	300
5	8	80	90	300
6	10	90	70	450
7	8	100	70	450
8	8	80	70	450
9	8	90	70	300
10	8	100	50	300
11	8	90	50	150
12	8	90	70	300
13	10	90	70	150
14	10	90	90	300
15	8	90	50	450
16	8	90	90	450
17	6	90	50	300
18	10	80	70	300
19	10	90	50	300
20	8	90	70	300
21	6	90	70	150
22	8	90	70	300
23	6	90	70	450
24	8	80	50	300
25	6	80	70	300
26	8	80	70	150
27	10	100	70	300
28	6	90	90	300
29	8	90	70	300

The optimization procedure for RSM mainly divided into three stages. The first stage is the selection of independent parameters and their levels. The second stage is the design the experimentation run and to get mathematical model equation. The third stage is obtaining the response surface plot, 3D and contour plot of response and determination of optimal process parameter setting [Rao, 2011]. A second-order regression model relating the response to the factors for BBD is given in Eq. (3.1).

$$Y = \beta_o + \sum_{i=1}^{k} \beta_i x_i + \sum_{i=1}^{k} \beta_{ii} x_i^2 + \sum_{i<j} \beta_{ij} x_i x_j \quad (3.1)$$

Where, Y is the response and xi (1, 2, ., k) are the independent k quantitative process variables. The coefficient β_O is a constant and β_i, β_{ii} and β_{ij} are the coefficients of linear, quadratic and interaction terms, respectively.

3.8 Taguchi based Fuzzy logic

Taguchi method involves reducing the variation in a process through robust design of experiments. Taguchi suggested that it is better to make a process robust than a machine. It is based on the fact that the effect of uncontrolled factors like (vibrations, noise, humidity etc.) can be reduced by the proper selection of the process parameters and their levels.

3.8.1 Design of Experiment

Design of experiment (DOE) is a structured, organized method that is used to determine the relationship between the different input factors that affecting a process and the output of that process. DOE requires only small set of experiments and helps to reduce time as well as cost of experiments. A total of 18 basic types of designed experimental matrixes were given by Taguchi (called as Orthogonal array (OA)). The selection of the OA is based on the number of input parameters (control factors), their levels and interactions between the parameters. For conducting the experiments, a L_{27} OA was chosen instead of L_9 OA to increase the sensitivity of experiments as shown in Table 3.7. The L_{27} orthogonal array has 13 columns that can be used to assign control factors and their interactions. The columns chosen for the control factors are 1, 2, 5 and 9.

Table 3.7: L27 Orthogonal array Experimental Design

	Factors			
Trail no	Gas Pressure	Power	Frequency	Feed
1	1	1	1	1
2	1	1	2	2
3	1	1	3	3
4	1	2	1	2
5	1	2	2	3
6	1	2	3	1
7	1	3	1	3
8	1	3	2	1
9	1	3	3	2
10	2	1	1	2
11	2	1	2	3
12	2	1	3	1
13	2	2	1	3
14	2	2	2	1
15	2	2	3	2
16	2	3	1	1
17	2	3	2	2
18	2	3	3	3
19	3	1	1	3
20	3	1	2	1
21	3	1	3	2
22	3	2	1	1
23	3	2	2	2
24	3	2	3	3
25	3	3	1	2
26	3	3	2	3
27	3	3	3	1

3.8.2 Determination of S/N ratio

The S/N ratio represents the degree of desirable to undesirable value of the process. The process parameter settings with maximum value of S/N ratio always give optimal quality with minimum scatter. The quality loss function may be of three types such as nominal-the-best, lower-the-better and higher-the-better type depending upon the nature of quality characteristics. In present research work, ‘smaller is the better’ principle was adopted to minimize the Kerf width, Kerf deviation and ‘larger is the better’ principle was adopted for Material removal rate.

Smaller is the better S/N ratio:

$$S/N = -10 \log\left(\frac{1}{r}\sum_{i=1}^{r} y_i^2\right) \tag{3.2}$$

Larger is the better S/N ratio:

$$S/N = -10 \log\left(\frac{1}{r}\sum_{i=1}^{r} \frac{1}{y_i^2}\right) \tag{3.3}$$

In Eq. (3.2) and (3.3), 'r' represents the number of experimental trails for same levels of process parameters and y_i is the experimental value of quality characteristics for ith experimental run.

3.8.3 Fuzzy logic approach

Fuzzy logic has a long history in mathematics and philosophy. It begins with the insight that not all statements are true or false to the some degree. Some claims are truer than others and so truth is a matter of degree. [Rajasekaran and Pai, 2010] The definition of performance characteristics such as lower-the-better, higher-the-better and nominal-the-better contains the degree of uncertainty and vagueness. Fuzzy logic has become a common tool to handle such information. Computers can only understand either '0' or '1', and 'MAX.' or 'MIN.'. Those data are called crisp or classic data and can be processed by all machines. In crisp logic, the truth values acquires 2-values, namely TRUE, FALSE which may be treated numerically equivalent to (0, 1). However, in fuzzy logic, truth values are multi-valued such as absolute true, partly true, absolute false, very true, very false, and so on and are numerically equivalent to (0, 1). Figure 3.8 shows the crisp and fuzzy sets.

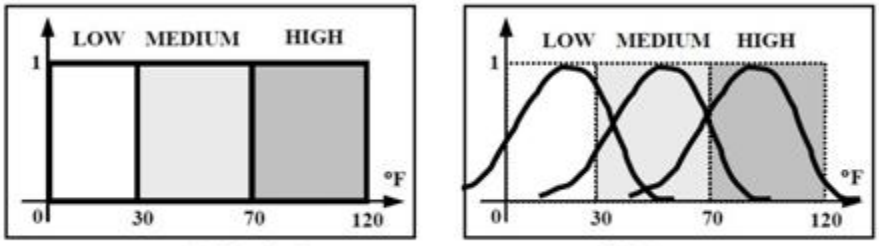

Figure 3.8: Representations of classical and fuzzy sets [Bai and Wang, 2006]

A fuzzy proposition is a statement which acquires a fuzzy truth values. Thus, given P to be a fuzzy proposition, T(P) represent the truth value (0-1) attached to P. In a simplest form, fuzzy propositions are associated with fuzzy sets.

Example

P: Gaurav is honest

T(P) = 0.8, if P is partly true

T(P) = 1, if P is absolute true

The Professor L. A. Zadeh invented the idea of fuzzy logic in 1965. Applications of fuzzy logic in industrial manufacturing, automatic control automobile production, banks, libraries, hospitals, and academic education rapid prototyping [Bai and Wang, 2006].

There are three main stages involves during the development of the model i.e. fuzzification (formation of membership function), fuzzy inference (expert rules), defuzzification as shown in Fig. 3.9.

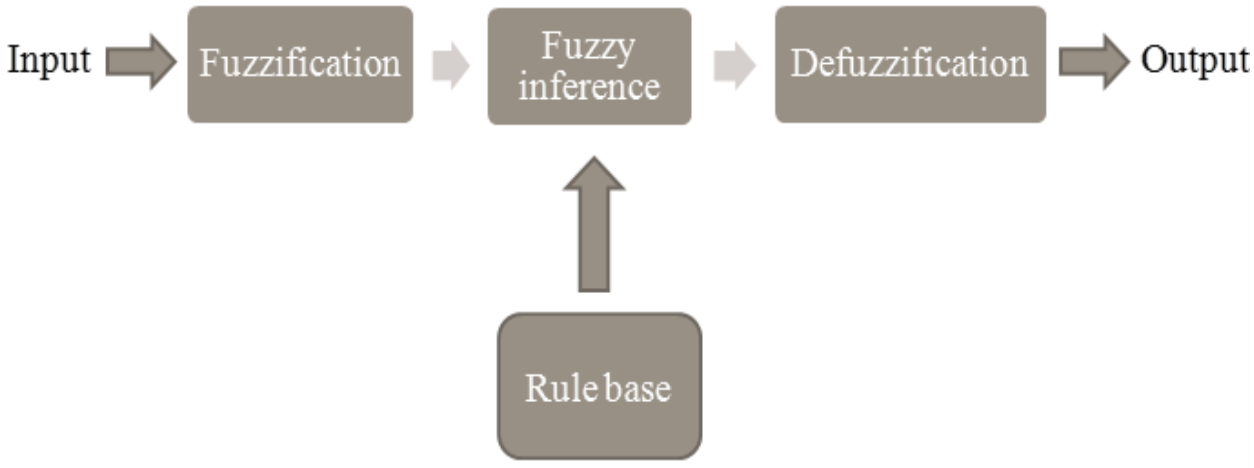

Figure 3.9: A fuzzy expert system [Bai and Wang, 2006]

Fuzzification

In fuzzification all input and output linguistic values are fuzzified with membership functions. The membership function defines how each input and output variable is mapped to membership value between 0 and 1. Proper selection of type of membership functions decides

the complexity and performance of fuzzy model. Triangular and trapezoidal membership functions are commonly used [Syn et al., 2011].

Membership function characterizes the fuzziness in graphical form. Types of membership function, such as

1) Triangular waveform
2) Trapezoidal waveform
3) Bell-shaped waveform
4) Gaussian waveform
5) S-curve waveform.

The selection of membership function depends on the actual applications. For those systems that need significant dynamic variation in a short period of time, a triangular or trapezoidal waveform should be utilized. Gaussian or S-curve waveform should be selected where very high control accuracy needed.

Fuzzy control rules

After the fuzzification, fuzzy inference rule base is formed. The rule base unit consists a series of fuzzy rules which describe the relationship between the input and output variables. The fuzzy rule base represents in the form of IF-THEN conditional statements. The IF part is mainly used to capture knowledge by using the elastic conditions whereas the THEN part can be utilized to give the conclusion or output in the form of linguistic variable.

For example:

Fuzzy expert rules

If ‘‘the prototype design’’ is ‘‘complicated’’ THEN ‘‘build up speed’’ is ‘‘long’’

Defuzzification

Defuzzification is the reverse method of fuzzification. Defuzzification refers to the method in which fuzzy output is converted into discrete value. Centroid method of Defuzzification is the most commonly used method.

Methods of defuzzification

1. Centroid method(centre of area)
2. Centre of sums
3. Mean of maxima

Chapter 4

Results and Discussion

4.1 Introduction

This chapter includes the result and discussion of experiments performed on fiber laser beam machine cutting of A653 Galvanized steel sheet. The main concern in laser beam cutting is to achieve the high cut quality which is not achieved by conventional process. The cut quality mainly depends on kerf width and kerf deviation. The objective of the study to determine the effect of laser cutting parameters like gas pressure, power, frequency and feed on quality characteristics like kerf width, kerf deviation, material removal rate and on metallurgical properties of material. Response surface methodology (RSM) technique was used to optimize the process parameters with considering the interactions and Taguchi based fuzzy logic technique was used to optimize the process parameters assuming no interaction between the factors.

4.2 Response surface methodology

Response surface methodology (RSM) is a collection of statistical and mathematical techniques. The Box-Behnken design was used for design the various experimentation run. Present work has been considered by taking four control factors at three levels, twenty nine experiments were performed on the basis of BBD design as shown in Table 4.1. This technique considers the effect of main factors as well as interaction effect on output responses. The effect of process parameters on each response is calculated by using mathematical model equation. The response surface plot, 3D and contour plot of response shows their nature of variation. The desirability approach is used for multi-response optimization. The percentage error is the difference between experimental and predicted value it shows the validation of the model. Design expert 6.0 software has been used to compute the values as shown in Table 4.1. Analysis of variance (ANOVA) has been performed to test the pertinence of the developed models and for establishing the mathematical relation between process parameters and response. ANOVA test designed to calculate the sum of squares of the response, F-value and lack of fit which shows the deviations of responses from the fitted surface [Ghosal and Manna, 2013]. The influence of

process parameters on surface topography, heat affected zone, recast layer and formation of cracks were analyzed by using microstructure analysis techniques i.e. scanning electron microscope (SEM) and energy dispersive spectroscopy (EDS).

Table 4.1: Design of experiments and results

Factors					Response Variables		
Standard Run no.	Gas pressure (kgf/cm2)	Power (W)	Frequency (Hz)	Feed (mm/min)	Kerf width (mm)	Kerf Deviation (mm)	MRR (mg/min)
1	8	90	90	150	0.241	0.272	280
2	6	100	70	300	0.358	0.375	602
3	8	100	70	150	0.336	0.348	278
4	8	100	90	300	0.347	0.267	545
5	8	80	90	300	0.349	0.238	611
6	10	90	70	450	0.405	0.348	760
7	8	100	70	450	0.421	0.281	802
8	8	80	70	450	0.396	0.278	487
9	8	90	70	300	0.462	0.391	541
10	8	100	50	300	0.378	0.297	608
11	8	90	50	150	0.362	0.325	267
12	8	90	70	300	0.469	0.372	530
13	10	90	70	150	0.356	0.385	338
14	10	90	90	300	0.395	0.253	693
15	8	90	50	450	0.387	0.324	675
16	8	90	90	450	0.401	0.248	667
17	6	90	50	300	0.370	0.326	615
18	10	80	70	300	0.382	0.367	685
19	10	90	50	300	0.414	0.416	490
20	8	90	70	300	0.472	0.378	505
21	6	90	70	150	0.320	0.389	219
22	8	90	70	300	0.468	0.397	520
23	6	90	70	450	0.372	0.351	664
24	8	80	50	300	0.377	0.371	314
25	6	80	70	300	0.346	0.387	334
26	8	80	70	150	0.319	0.357	267
27	10	100	70	300	0.408	0.367	511
28	6	90	90	300	0.336	0.302	321
29	8	90	70	300	0.489	0.383	550

4.2.1 Effect of process parameters on Kerf Width

There are many process parameters which affects the edge quality in terms of kerf width. In the present research work, the kerf width (K_w) measured by taking the average of five locations on each cut along the length of cut. The exothermic oxidation reaction decides the edge quality which directly depends on the input parameters like gas pressure, laser power, feed rate etc. The appropriateness of model and effects of process parameters with their interactions for Kerf width have been shown in ANOVA Table 4.2. The Model F-value of 54.58 implies the model is significant. This model was developed for 95% confidence level. There is only a 0.01% chance that a "Model F-Value" this large could occur due to noise. Values of "Prob > F" less than 0.0500 indicate model terms are significant. In this case A, C, D, A^2, B^2, C^2, D^2, CD are significant model terms. Values greater than 0.1000 indicate the model terms are not significant. The "Lack of Fit F-value" of 1.72 implies the Lack of Fit is not significant relative to the pure error. It can be observed from the F and P values that the factors D (Feed) and A (Gas pressure) have more significant effect on Kerf width.

Table 4.2: The analysis of variance for main and interaction effect of parameters on Kerf width

Source	Sum of Squares	DOF	Mean Square	F value	Prob > F	At 95% CI
Model	0.0797	9	0.0089	54.58	< 0.0001	Significant
A	0.0055	1	0.0055	34.19	< 0.0001	Significant
B	0.0005	1	0.0005	3.21	0.0893	not significant
C	0.0040	1	0.0040	24.64	< 0.0001	Significant
D	0.0167	1	0.0167	103.10	< 0.0001	Significant
A2	0.0125	1	0.0125	77.12	< 0.0001	Significant
B2	0.0159	1	0.0159	98.14	< 0.0001	Significant
C2	0.0211	1	0.0211	130.10	< 0.0001	Significant
D2	0.0251	1	0.0251	154.53	< 0.0001	Significant
CD	0.0046	1	0.0046	28.09	< 0.0001	Significant
Lack of Fit	0.0027	15	0.0002	1.72	0.3195	not significant
R^2 = 0.9628						
R^2 Adjusted = 0.9451						
R^2 Predicted = 0.8896						

The "Pred R-Squared" of 0.8896 is in reasonable agreement with the "Adj R-Squared" of 0.9451. "Adeq Precision" measures the signal to noise ratio. A ratio greater than 4 is desirable. "Adeq Precision" ratio of 27.883 indicates an adequate signal. Regression equation shows the mathematical relationship between different operating parameters and kerf width with the help of second order polynomial model. Final equation in terms of coded factors.

$$\text{Kerf Width} = 0.47 + 0.022 \times A + 0.007 \times B - 0.018 \times C + 0.037 \times D - 0.044 \times A^2 - 0.050 \times B^2 - 0.057 \times C^2 - 0.062 \times D^2 + 0.034 \times CD$$

Final Equation in terms of actual factors:

$$\text{Kerf Width} = -5.111 + 0.1864 \times \text{Gas Pressure} + 0.0898 \times \text{Power} + 0.0157 \times \text{Frequency} + 0.0011 \times \text{Feed} - 0.011 \times \text{Gas Pressure}^2 - 0.0005 \times \text{Power}^2 - 0.0001 \times \text{Frequency}^2 - 0.000003 \times \text{Feed}^2 + 0.000011 \times \text{Frequency} \times \text{Feed}$$

Effect of main factors on kerf width

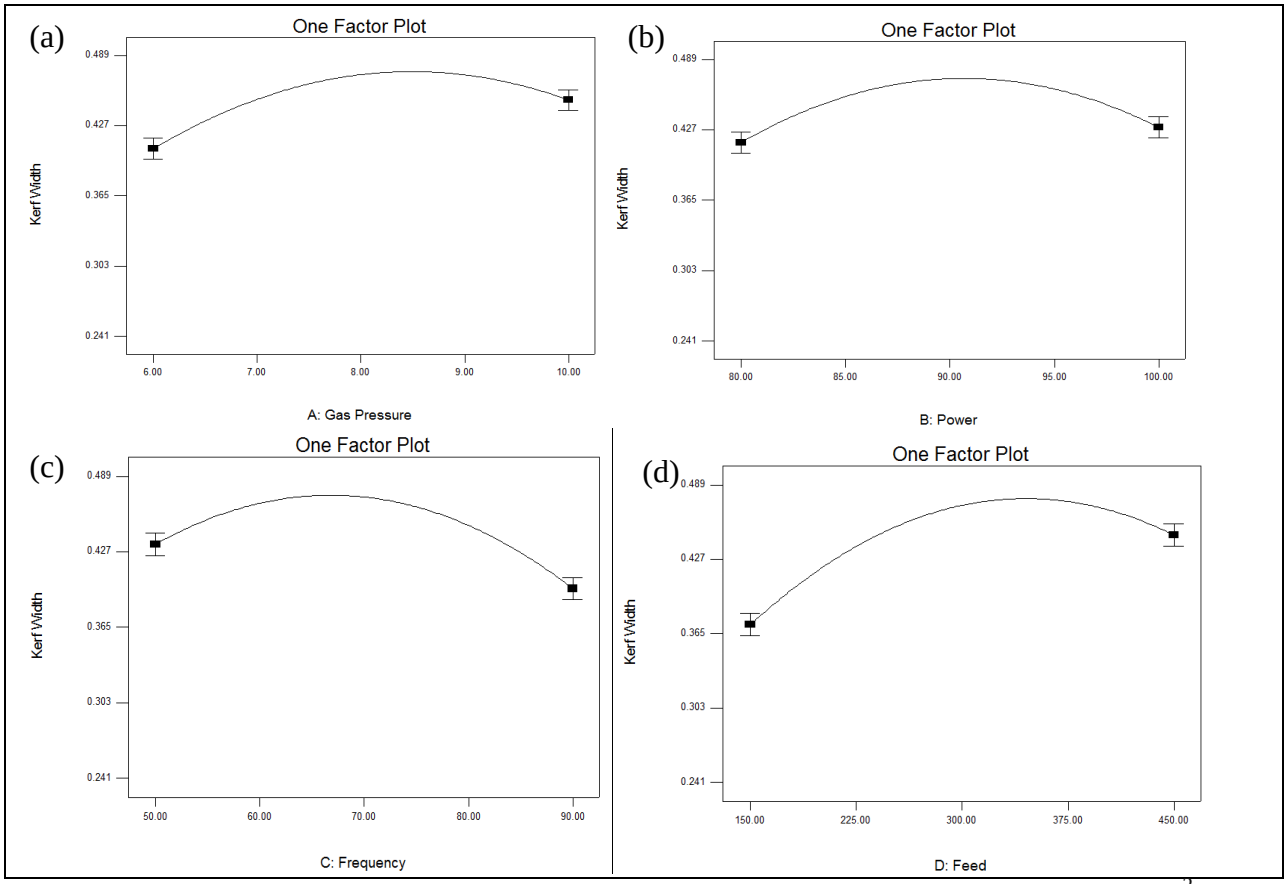

Figure 4.1: Main factors plot on kerf width (a) Gas pressure varied from 6 to 10 kgf/cm^2 at power = 90 W, frequency = 70 Hz, feed = 300 mm/min. (b) Power varied from 80 to 100 W at gas pressure = 8 kgf/cm^2, frequency = 70 Hz, feed = 300 mm/min. (c) Frequency varied from 50 to 90 Hz at gas pressure = 8 kgf/cm^2, power = 90 W, feed = 300 mm/min. (d) Feed varied from 150 to 450 mm/min at gas pressure = 8 kgf/cm^2, power = 90 W, frequency = 70 Hz.

From the main effect plots, as shown in Fig. 4.1 (a) it can be observed that when gas pressure increased from 6 to 10 kgf/cm^2 the kerf width size increased from 0.407 to 0.450 mm. It is caused due to the fact that as gas pressure increases, the melt flow velocity of molten material increases which blows away more molten material from the cutting region. Meanwhile, when power increased from 80 to 100W the kerf width size increased from 0.416 to 0.430 mm as shown in Fig. 4.1 (b). This can be explained by as the power increases, the laser beam density increases so, high amount of heat produced melts or vaporizes the more material at focused zone and increase the width of the cut. Further, when initially frequency increases from 50 to 70 Hz the kerf width value increases from 0.433 to 0.472 mm and then after further increases in frequency from 70 to 90 Hz the value of kerf width start decreasing from 0.472 to 0.397 mm as shown in Fig. 4.1 (c). The variation in kerf width was not seen much when power increased, which resulted into non-significant parameter.

Determination the effect of interactions on kerf width

It can be seen from the ANOVA Table 4.2 that the interaction between frequency and feed is significant. Figure 4.2 (b) and (c) shows the three-dimensional interaction response surfaces and contour plots for the response Kerf width. From the contour plot and response surface plot, it was observed that kerf width value increases from 0.299 to 0.472 mm with the increase in feed from 150 to250 mm/min and decrease of frequency from 90 to 50 Hz. The Kerf width value decreases on increasing the frequency and decreasing feed. The interaction plot of frequency and feed on kerf width is shown in Fig. 4.2 (a). From Fig. 4.2 (d) to Fig. 4.2 (f) shows the normal plot of residuals, predicted versus actual and residuals versus run. It was found that the residuals generally fall along the straight line and points are close to each other implying that the errors are normally distributed. Figure 4.2 (d) shows the points in normal plot of residuals are along the straight line and points are close to each other implying that the error terms are normally distributed. The graph between the predicted value and actual value shows the accuracy of model is shown in Fig. 4.2 (e). The residual shows the difference between actual value and predicted value.

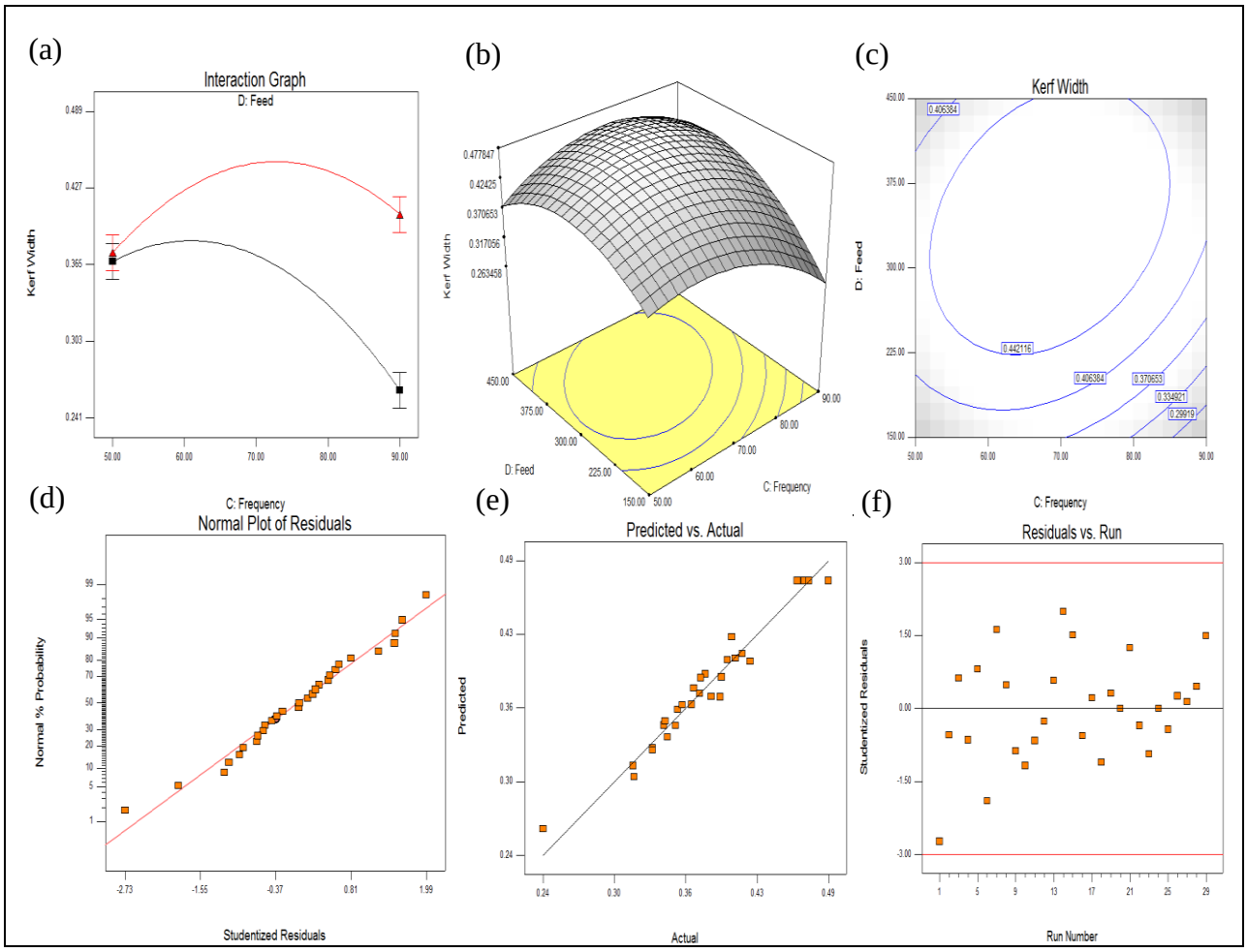

Figure 4.2: Response surface plots of Kerf width (a) interaction plot, (b) 3D surface and (c) contour plot between frequency and feed at gas pressure = 8 kgf/cm^2, power = 90 W, (d) normal plot of residuals, (e) relation between actual and predicted value and (f) residuals versus run.

4.2.2 Effect of process parameters on Kerf Deviation

The kerf deviation shows the uniformity of the length of cut. To achieve high accuracy in cutting the kerf deviation always should kept as small as possible. Kerf deviation is the difference of maximum KW and minimum KW measured along the length of cut.

Kerf deviation = (Maximum kerf width-Minimum kerf width) (1)

Table 4.3 shows the ANOVA for main and interaction effects of parameters on Kerf deviation. Based on ANOVA frequency, feed and two interaction gas pressure and frequency (AC), power and frequency (BC) are significant for kerf deviation. This model was developed for 95% confidence level. The Model F-value of 27.99 implies the model is significant. Values

of "Prob > F" less than 0.0500 indicate model terms are significant. In this case C, D, A^2, B^2, C^2, D^2, AC, BC are significant model terms.

Table 4.3: Analysis of variance for main and interaction effect of parameters on Kerf deviation

Source	Sum of Squares	DOF	Mean Square	F Value	Prob > F	At 95% CI
Model	0.070	10	0.007	27.99	< 0.0001	Significant
A	0.000	1	0.000	0.01	0.9139	not significant
B	0.000	1	0.000	1.33	0.2646	not significant
C	0.019	1	0.019	76.66	< 0.0001	significant
D	0.005	1	0.005	20.22	0.0003	significant
A2	0.001	1	0.001	4.50	0.0481	significant
B2	0.005	1	0.005	21.09	0.0002	significant
C2	0.028	1	0.028	110.65	< 0.0001	significant
D2	0.007	1	0.007	26.38	< 0.0001	significant
AC	0.005	1	0.005	19.37	0.0003	significant
BC	0.003	1	0.003	10.63	0.0043	significant
Lack of Fit	0.004	14	0.000	2.93	0.1544	not significant
R^2 = 0.9396						
R^2 Adjusted = 0.9060						
R^2 Predicted = 0.8209						

The "Lack of Fit F-value" of 2.93 implies the Lack of Fit is not significant relative to the pure error. There is a 15.44% chance that a "Lack of Fit F-value" this large could occur due to noise. It was observed from the F and P values that the frequency has a most significant effect on Kerf deviation. The "Pred R-Squared" of 0.8209 is in reasonable agreement with the "Adj R-Squared" of 0.9060. The regression equation for the kerf deviation was modelled as follows Final Equation in Terms of Coded Factors:

Kerf deviation = 0.38 +0.0005 × A -0.005 × B -0.040 × C -0.021 × D +0.013 × A^2 -0.028 × B^2 -0.065 × C^2 -0.032 × D^2 -0.035 × AC +0.026 × BC

Kerf deviation = -2.088+0.0085 × Gas Pressure +0.0417 × Power +0.0162 × Frequency +0.0007 × Feed +0.0033 × Gas Pressure^2 -0.0003 × Power^2 -0.0002 × Frequency^2 -0.000001 × Feed^2 -0.0009 × Gas Pressure × Frequency +0.0001 × Power × Frequency

Effect of main factors on kerf Deviation

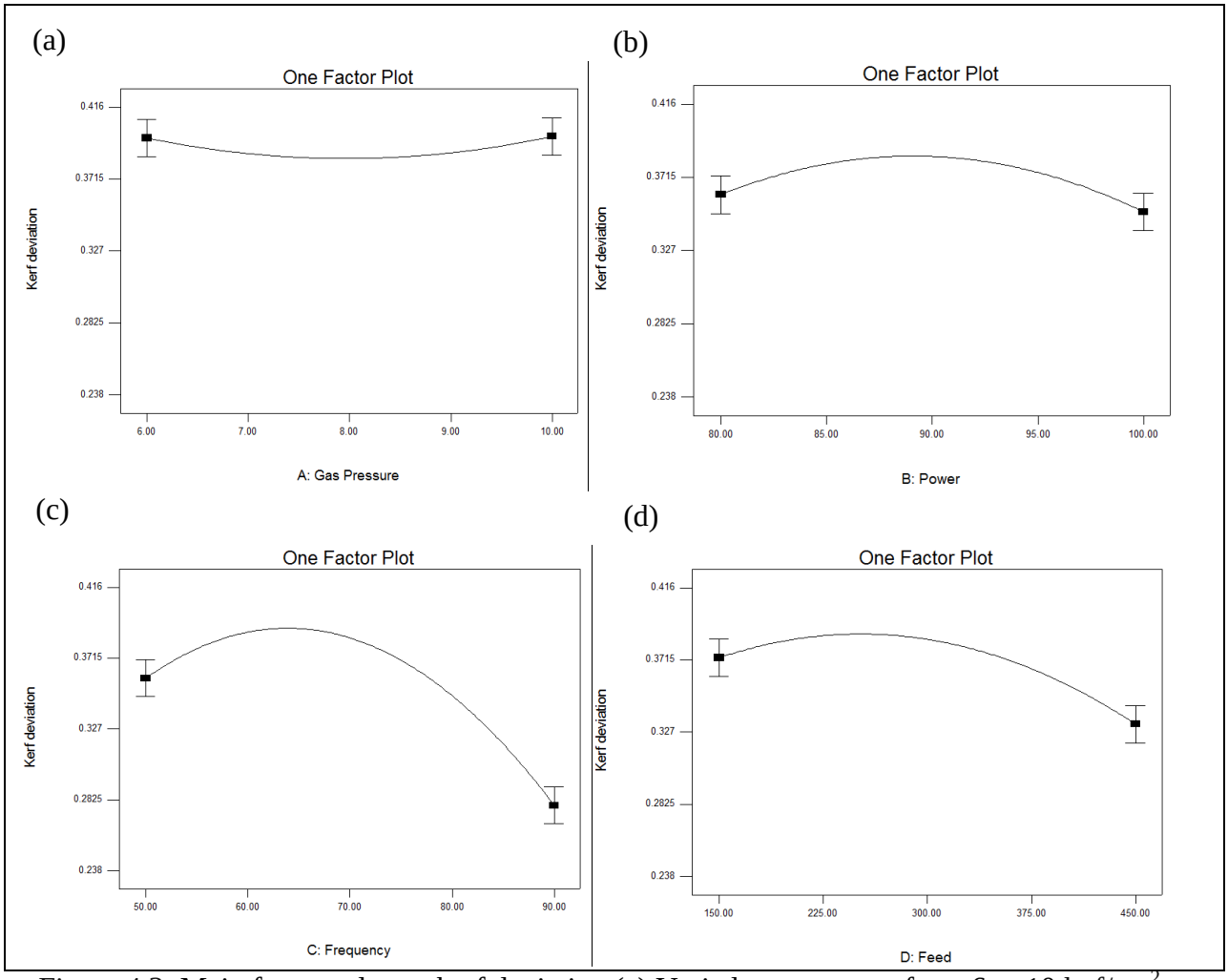

Figure 4.3: Main factors plot on kerf deviation (a) Varied gas pressure from 6 to 10 kgf/cm^2 at power = 90 W, frequency = 70 Hz, feed = 300 mm/min. (b) Varied power from 80 to 100 W at gas pressure = 8 kgf/cm^2, frequency = 70 Hz, feed = 300 mm/min. (c) Varied frequency from 50 to 90 Hz at gas pressure = 8 kgf/cm^2, power = 90 W, feed = 300 mm/min. (d) Varied feed from 150 to 450 mm/min at gas pressure = 8 kgf/cm^2, power = 90 W, frequency = 70 Hz.

It was observed from Fig. 4.3 (c) that when frequency increased from 50 to 90 Hz the kerf deviation value decreased from 0.359 to 0.279 mm. The variation in kerf deviation was not seen much when gas pressure and power increased, which resulted into non-significant parameters as shown in Fig. 4.3 (a) and (b). Further, when feed increased from 150 to 450 mm/min the value of kerf deviation was decreased from 0.373 to 0.332 mm as shown in Fig. 4.3 (d). This can be explained on the fact that as feed increases, the interaction time between laser beam and material reduces significantly, which results into less unevenness in kerf.

Determination the effect of interactions on kerf Deviation

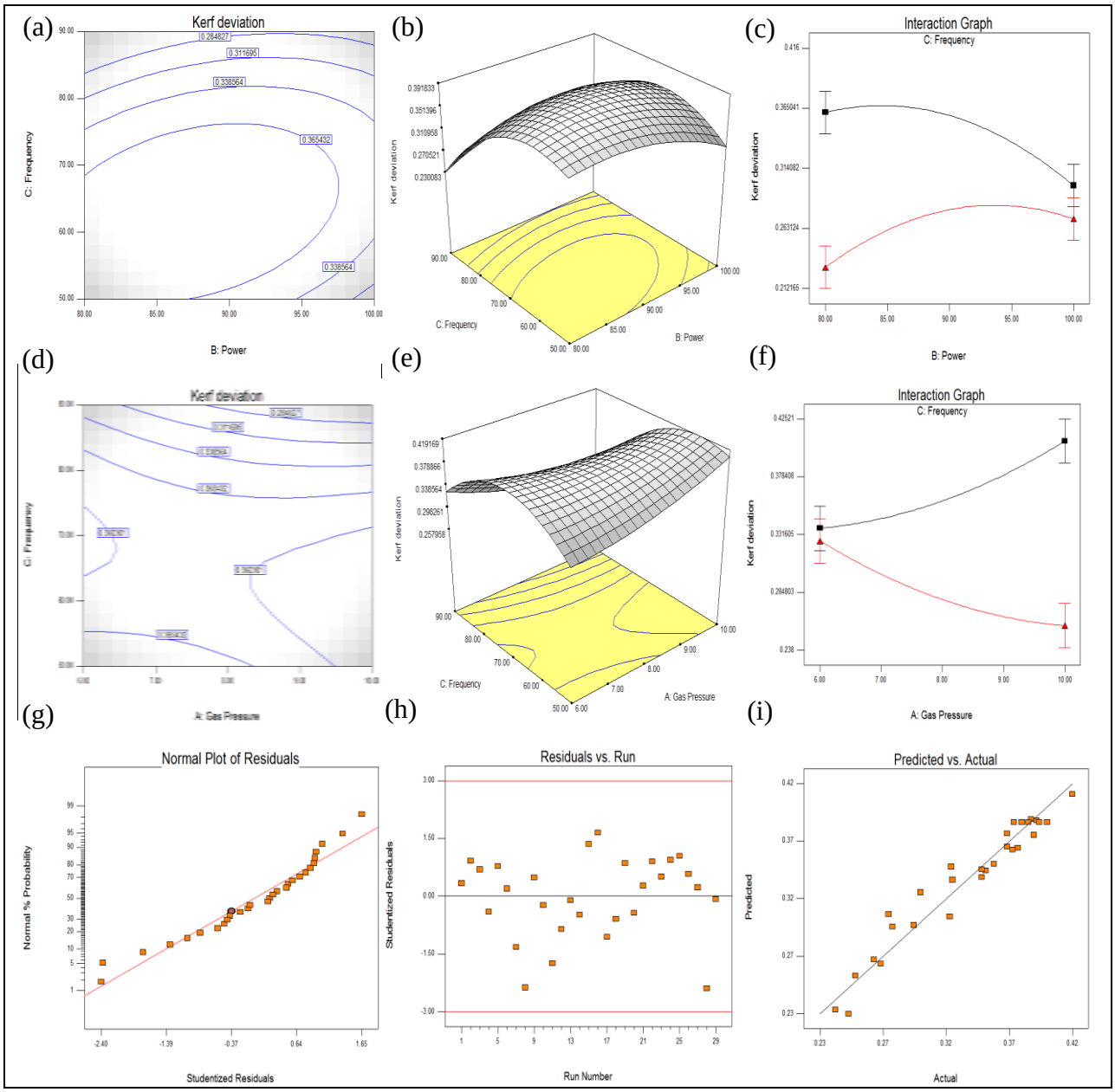

Figure 4.4: Response surface plots of Kerf deviation (a) contour plot, (b) 3D surface and (c) interaction plot between frequency and power at gas pressure = 8 kgf/cm^2, feed = 300 mm/min, (d) contour plot, (e) 3D surface and (f) interaction plot between frequency and gas pressure at power = 90 W, feed = 300 mm/min, (g) normal plot of residuals, (h) residuals versus run (i) relation between actual and predicted value.

The kerf deviation value also depends on the interaction of different parameters. From Fig. 4.4 (a) to Fig. 4.4 (f) shows the contour plots and three-dimensional interaction response surfaces for the response Kerf deviation. From the contour plot and three-dimensional surface

plot of power and frequency, it was observed that kerf deviation value increased from 0.285 to 0.384 mm with the decrease in frequency from 90 to 50 Hz and decrease of power from 100 to 80 W as shown in Fig. 4.4 (a) and (b). The kerf deviation value increases with increase in gas pressure and decrease in frequency as shown in Fig. 4.4 (d) and (e). Figure 4.4 (g) to Fig. 4.4 (i) displays the normal plot of residuals, residuals versus run and predicted versus actual for kerf deviation. It was found that points are close to each other implying that the errors are normally distributed. Distribution of the data is random. Residuals do not contradict the linear assumption.

4.2.3 Effect of process parameters on MRR

The MRR (mg/min) was calculated as:

MRR= (Loss of mass during each cut × cutting speed) / length of cut (2)

The loss of mass was calculated by weighing the specimen before and after cutting using CAS Electronics balance (CAY 220). The machine has least count of 0.1 mg and maximum capacity of 220 gm. Based on analysis of variance (ANOVA) as shown in Table 4.4, Gas pressure, power, feed and four interactions are significant to MRR.

Table 4.4: The analysis of variance for main and interaction effect of parameters on MRR

Source	Sum of Squares	DOF	Mean Square	F Value	Prob > F	At 95% CI
Model	747780	9	83087	57.32	< 0.0001	Significant
A	43335	1	43335	29.90	< 0.0001	Significant
B	34975	1	34975	24.13	< 0.0001	Significant
C	1842	1	1842	1.27	0.2737	not significant
D	482411	1	482411	332.83	< 0.0001	Significant
D2	19415	1	19415	13.39	0.0017	Significant
AB	48720	1	48720	33.61	< 0.0001	Significant
AC	61554	1	61554	42.47	< 0.0001	Significant
BC	32400	1	32400	22.35	0.0001	Significant
BD	23130	1	23130	15.96	0.0008	Significant
Lack of Fit	26296	15	1753	5.64	0.0534	not significant
R^2 = 0.9645						
R^2 Adjusted = 0.9477						
R^2 Predicted = 0.8811						

This model was developed for 95% confidence level. The Model F-value of 57.32 implies the model is significant. Values of "Prob > F" less than 0.0500 indicate model terms are significant. In this case A, B, D, D^2, AB, AC, BC, BD are significant model terms. Values greater than 0.1000 indicate the model terms are not significant. The "Lack of Fit F-value" of 5.64 implies there is a 5.34% chance that a "Lack of Fit F- value" this large could occur due to noise. The "Pred R-Squared" of 0.8811 is in reasonable agreement with the "Adj R-Squared" of 0.9477. "Adeq Precision" measures the signal to noise ratio. A ratio greater than 4 is desirable. Your ratio of 26.441 indicates an adequate signal. It was observed from the F and P values that the feed has a most significant effect on MRR. The relationship between various machining factors and MRR is represented as follows regression equation in form of second-order polynomial model.

Final Equation in Terms of Coded Factors:

$$MRR = 527.98 + 60.09 \times A + 53.99 \times B + 12.39 \times C + 200.50 \times D - 52.54 \times D^2 - 110.36 \times AB + 124.05 \times AC - 90.00 \times BC + 76.04 \times BD$$

Final Equation in Terms of Actual Factors:

$$MRR = -4555.36 + 309.59 \times \text{Gas Pressure} + 65.84 \times \text{Power} + 16.31 \times \text{Frequency} - 1.83 \times \text{Feed} - 0.002 \times \text{Feed}^2 - 5.52 \times \text{Gas Pressure} \times \text{Power} + 3.10 \times \text{Gas Pressure} \times \text{Frequency} - 0.45 \times \text{Power} \times \text{Frequency} + 0.051 \times \text{Power} \times \text{Feed}$$

Effect of main factors on MRR

It was observed from Fig. 4.5 (a) to Fig. 4.5 (d) that when gas pressure, power, frequency and feed increases the value of MRR increase. The value of MRR is directly proportional to control factors. The variation in MRR was not seen much when frequency increased, which resulted into non-significant parameter. From the main plot in Fig. 4.5 (a), it can be analysed that as gas pressure value increases from 6 to 10 kgf/cm^2 the MRR value increases from 467.8 to 588 mg/min. Further, when feed was increased from 150 to 450 mm/min the value of MRR increased from 275 to 676 mg/min as shown in Fig. 4.5 (d). It is caused due to the fact that as feed rate increases, the laser cutting speed increases so material cut very fast and laser cover more distance in less time.

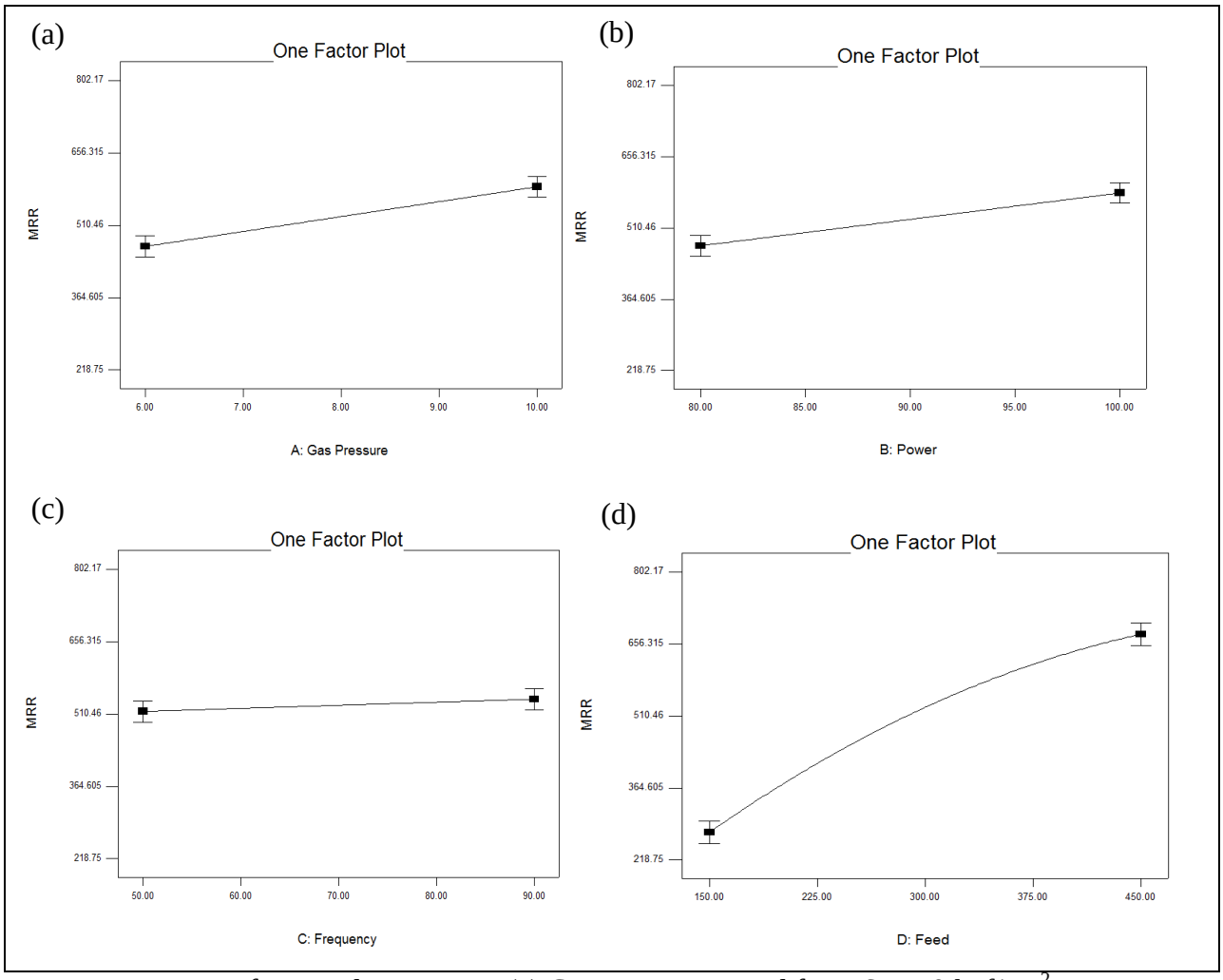

Figure 4.5: Main factors plot on MRR (a) Gas pressure varied from 6 to 10 kgf/cm^2 at power = 90 W, frequency = 70 Hz, feed = 300 mm/min. (b) Power varied from 80 to 100 W at gas pressure = 8 kgf/cm^2, frequency = 70 Hz, feed = 300 mm/min. (c) Frequency varied from 50 to 90 Hz at gas pressure = 8 kgf/cm^2, power = 90 W, feed = 300 mm/min. (d) Feed varied from 150 to 450 mm/min at gas pressure = 8 kgf/cm^2, power = 90 W, frequency = 70 Hz.

Determination the effect of interactions on MRR

From Fig. 4.6 (a) to Fig. 4.6 (f) shows the response surface interaction plots, contour plots and three-dimensional interaction response surfaces for the response MRR. From the contour plot and three-dimensional surface plot as shown in Fig. 4.6 (b) and (c), it can be observed that MRR value increases from 360.35 to 587.63 mg/min with increase in gas pressure from 6 to 10 kgf/cm^2 and power from 80 to 100 W. This can be explained as gas pressure increased the melt flow velocity of molten material increased higher MRR.

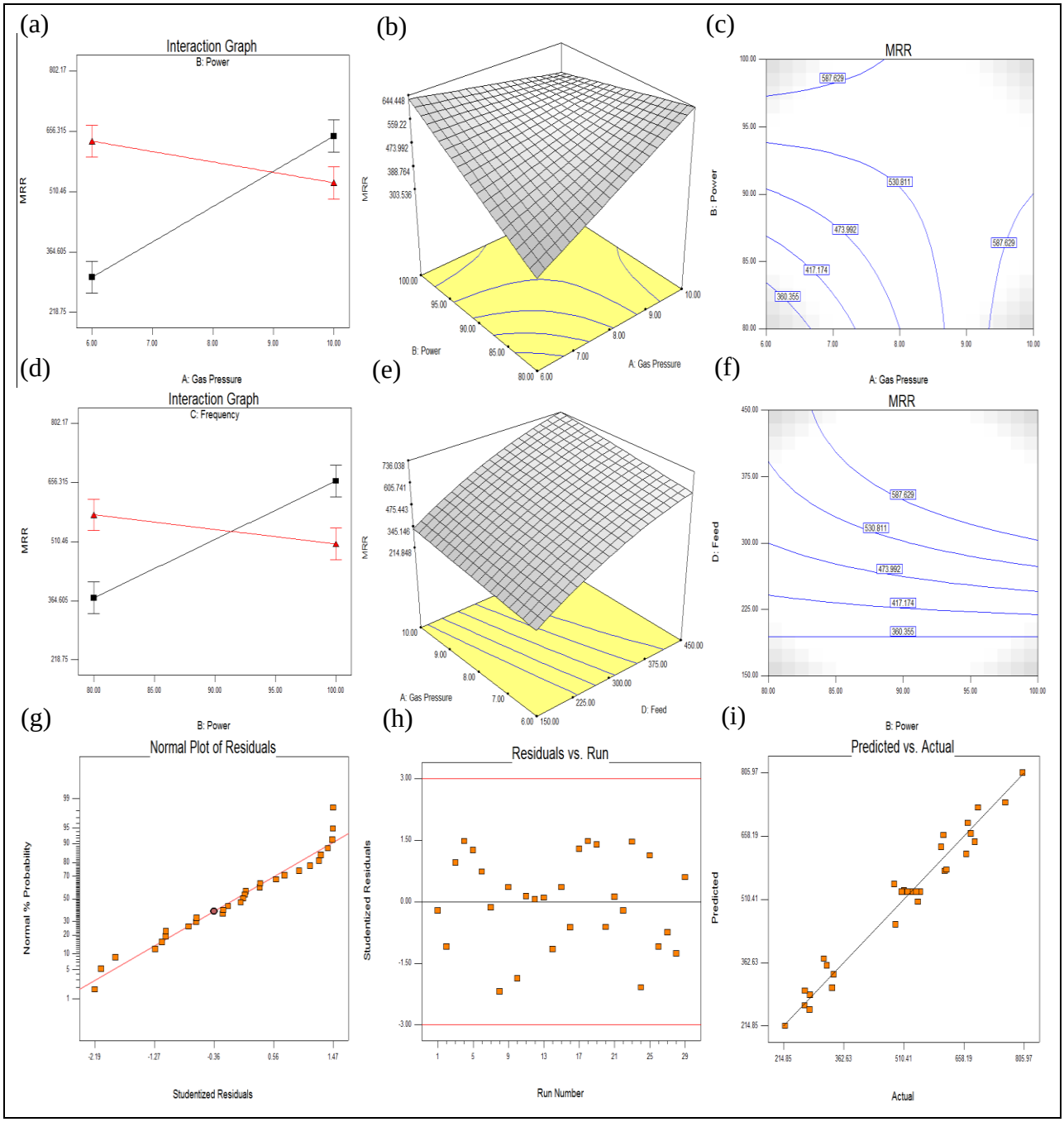

Figure 4.6: Response surface plots of MRR (a) interaction plot, (b) 3D surface and (c) contour plot between power and gas pressure at frequency = 70 Hz, feed = 300 mm/min, (d) interaction plot between frequency and power, (e) 3D surface interaction plot between gas pressure and feed (f) contour plot between feed and power at gas pressure = 8 kgf/cm^2, frequency = 70 Hz, (g) normal plot of residuals, (h) actual versus predicted value, (i) residuals versus run.

Further, when feed and power increased from 150 to 450 mm/min and 80 to 100 W respectively the value of MRR increases as shown in Fig. 4.6 (f). It is caused due to the fact that increase in power cause increase in beam energy density and increase in feed cause increases laser cutting speed, so their interaction effect overall increase in MRR. Three-dimensional interaction response surface for gas pressure and feed shows the increasing trend of MRR with increase in gas pressure and feed as shown in Fig. 4.6 (e). Figure 4.6 (g) shows the normal plot of residuals, Residuals generally fall along the straight line implying that the error terms are normally distributed. It was found that the experimental results are very close to the predicted values as shown in Fig. 4.6 (i) predicted versus actual. The graph between the predicted value and actual value shows the accuracy of model.

4.2.4 Surface Topography

LBM is a thermal energy based process, it produces heat affected zone, recast layer and thermal stress in the material. The present research work mainly investigate the influence of process parameters or conditions on surface topography, recast layer, heat affected zone and formation of cracks were analyzed by using Scanning electron microscope (SEM) and energy dispersive spectroscopy (EDS). The material is removed by laser beam which produces high amount of heat thus vaporizes or melts the material. The rise in temperature cause to change in material microstructure and change it's grain size. Development of thermal stresses results in Crack formation as well as plastic deformation. A good relationship has been developed between surface properties and their associated modes of failure. Surface roughness is mainly responsible for affecting fatigue strength because, with an increment in the roughness of the surface, correspondingly decrement in fatigue life is observed [Kumar et al., 2013a]. In order to sustain in this, competitive world every industry must strive to produce good quality product to the customer at a minimal rate. Through good surface morphology product's precision as well as quality of conformance are greatly enhanced.

Scanning electron microscope analysis

Scanning electron microscope (SEM) analysis is basically a widely adopted method for evaluating the surface characteristics of different materials. Electron beam is made to impinge over the test specimen for evaluation of its surface characteristic through the image obtained.

SEM produces very high magnification images ranging from 10 to 50000 times and at high resolution up to 2 nm combined with the ability to generate localised chemical information (EDS) [Balasubramaniam, 2014].

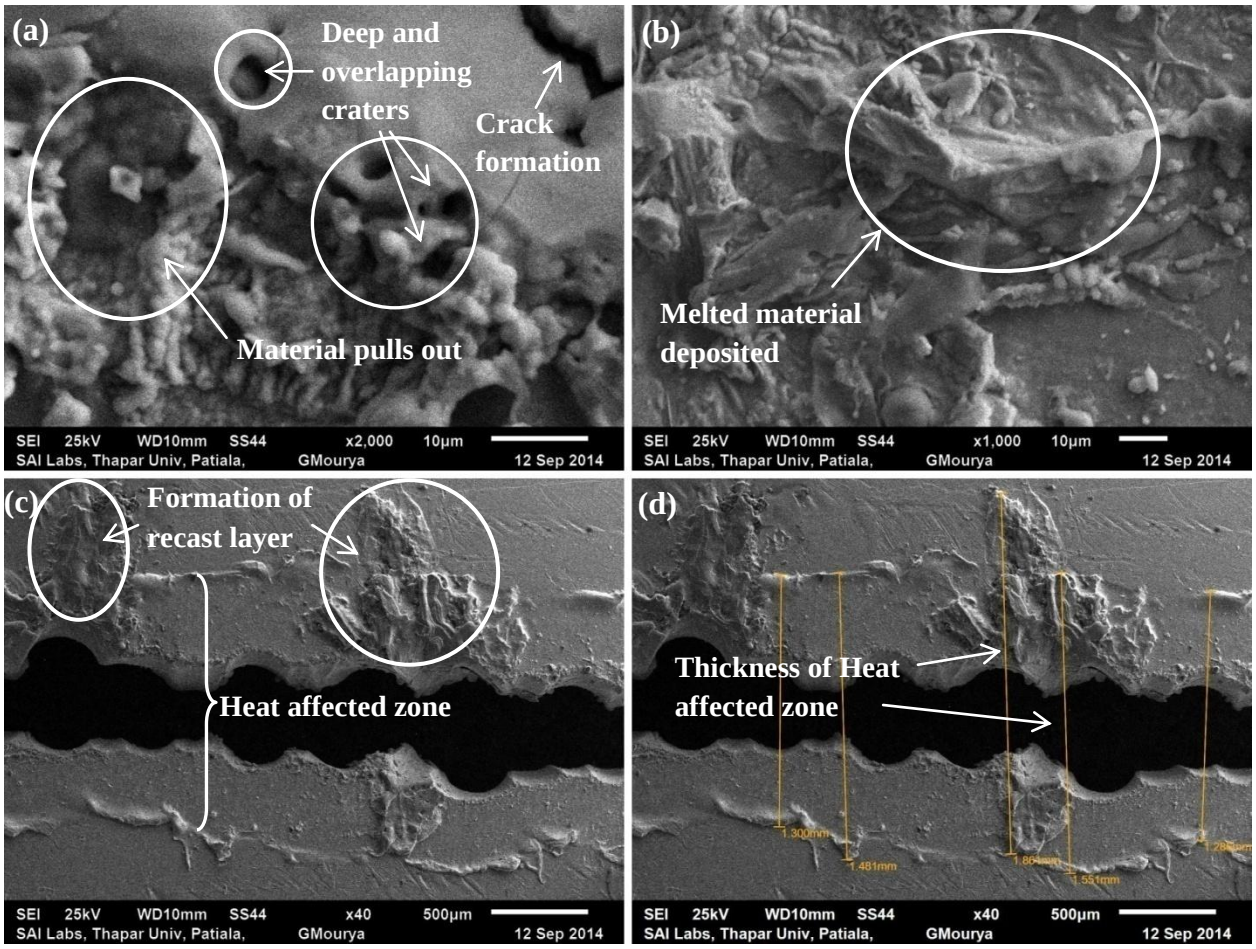

Figure 4.7: SEM micrographs at Gas pressure = 6 Kgf/cm^2, power = 90 W, frequency = 70 Hz, feed = 150 mm/min. (a) Deep and overlapping craters, material pulls out and micro cracks (2000×) (b) Melted material deposited (1000×) (c) Heat affected zone and recast layer formation (d) Average thickness of HAZ.

From the surface texture as shown in Fig. 4.8, it can observe that the formation of craters, lumps of debris and recast layer reduced as compare to Fig. 4.7. It was observed that as gas pressure increases from 6 kgf/cm^2 to 10 kgf/cm^2 the formation of recast layer decreases. The reason behind it as gas pressure increases more molten material blows away from the cutting zone so very less material left to resolidified to form recast layer. The size of recast layer mainly depends on gas pressure. The value of MRR also increased as more material move away and increase in feed. The value of kerf width, kerf deviation and MRR for the Fig. 4.8 at (Gas

pressure = 10 Kgf/cm^2, power = 90 W, frequency = 70 Hz, feed = 450 mm/min) were 0.405 mm, 0.348 mm and 760 mg/min respectively and the average thickness value of HAZ was 0.520 mm. It was found that HAZ value decreases from 1.20 to 0.520 mm with increase in feed from 150 to 450 mm/min due to the contact time between work material and laser beam shortened greatly, which results in less HAZ.

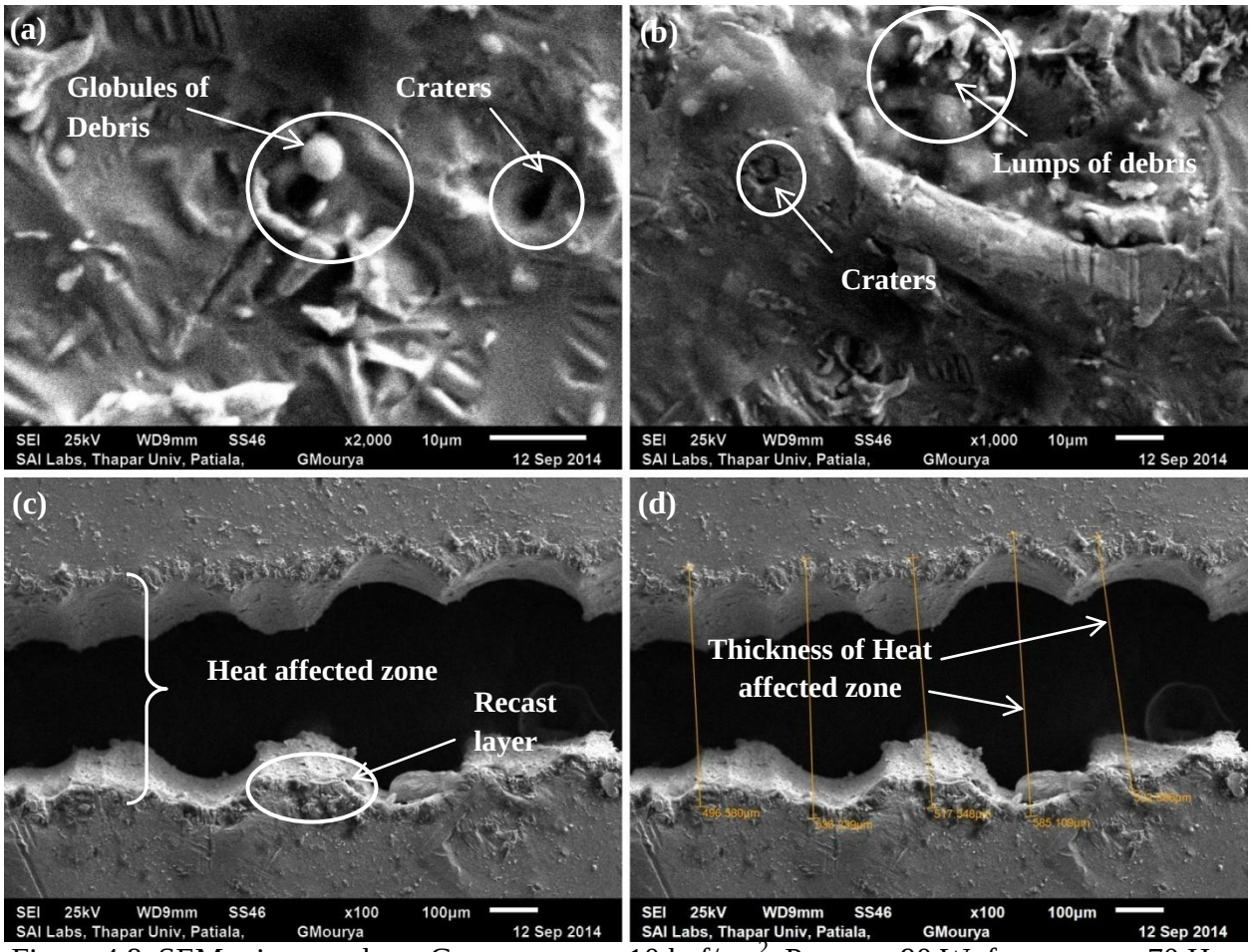

Figure 4.8: SEM micrographs at Gas pressure = 10 kgf/cm^2, Power = 90 W, frequency = 70 Hz, feed = 450 mm/min. (a) less no of Craters, globules of debris and cracks (2000×) (b) Lumps of debris (1000×) (c) Heat affected zone and recast layer (d) Thickness of HAZ.

It was analyzed as power and frequency increased during laser machining process the high amount of high energy released lead to formation of globules of debris, craters, pull of material and deep and wide craters as shown in Fig. 4.9 (a) and (b). The formation of recast layer increased as gas pressure decreased from 10 to 8 kgf/cm^2 and power increased from 90 to 100 W as shown in Fig. 4.9 (c). It can be seen from Fig. 4.9 (c) that recast layer emerges as non-uniform pattern. The value of kerf width, kerf deviation and MRR for the Fig. 4.9 at (Gas pressure = 8

kgf/cm^2, power = 100 W, frequency = 90 Hz, feed = 300 mm/min) were 0.347 mm, 0.267 mm and 545 mg/min respectively and the average thickness value of HAZ was 1.35 mm. it was observed that HAZ value increased from 0.520 to 1.35 mm with increase in power from 90 to 100 W and frequency increase from 70 to 90 Hz.

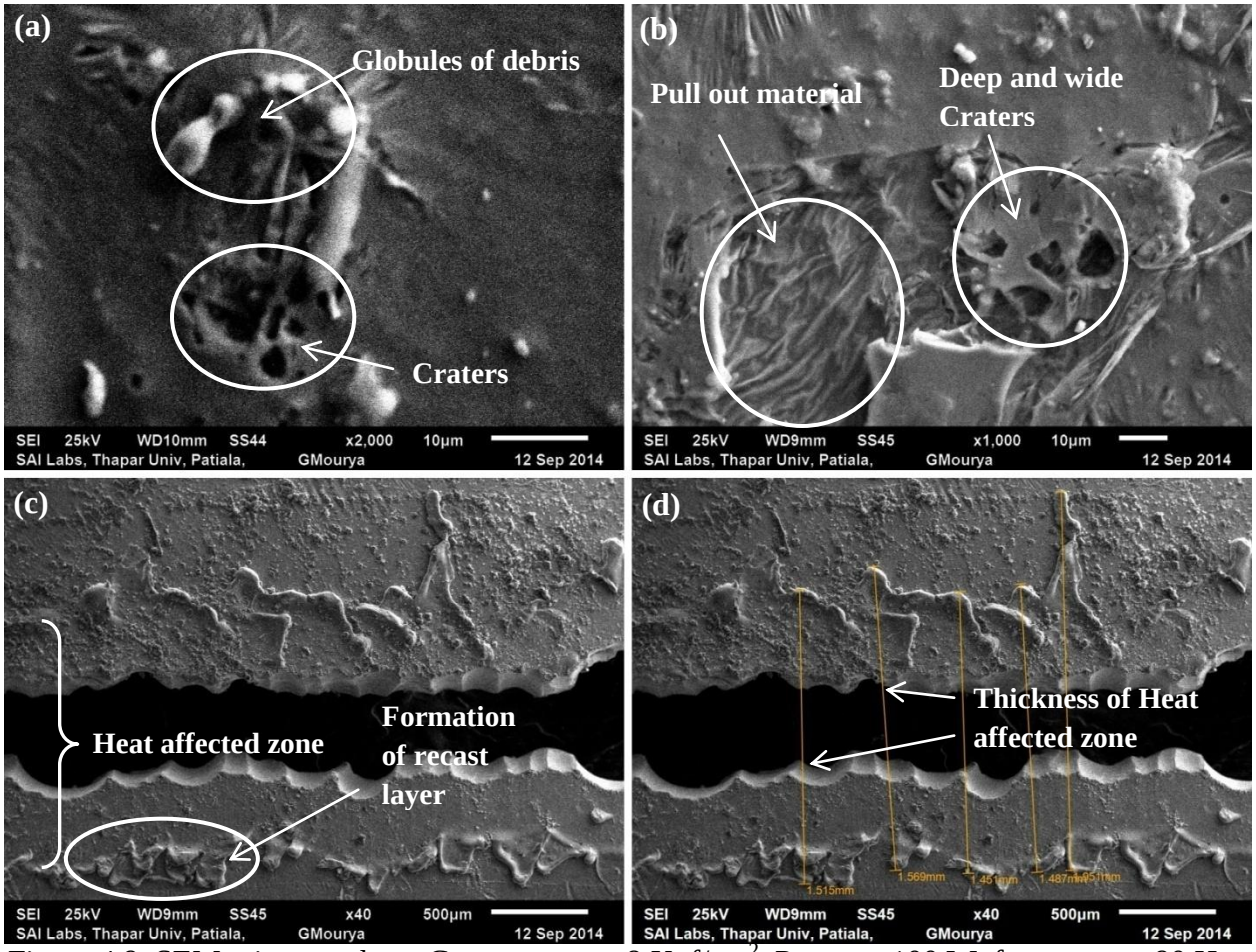

Figure 4.9: SEM micrographs at Gas pressure = 8 Kgf/cm^2, Power = 100 W, frequency = 90 Hz, feed = 300 mm/min. (a) Craters and globules of debris (2000×) (b) Pull out material, deep and wide craters (1000×) (c) Heat affected zone and recast layer (d) Average thickness of HAZ.

It was found that increase in power and frequency led to increase in HAZ value. Power and frequency have significant effect on HAZ. This can be explained by as the power and frequency increases, the intensity of laser beam increases so, excessive amount of heat produced and transmit to surrounding of cutting region. It changes the microstructure and properties of affected region known as Heat affected zone.

Energy dispersive spectroscopy Analysis

Various elemental composition of material are determine through an output in the form of image obtain from the EDS. EDS is a scientific technique used to determine the elemental composition of machined samples. An output of EDS is dependent on the X-ray received for an each level of energy. It is based on the fundamental principle of each element has a unique atomic structure and unique set of peaks [Kumar et al., 2013a]. Figure 4.10 shows the detected elemental composition of laser machined surface.

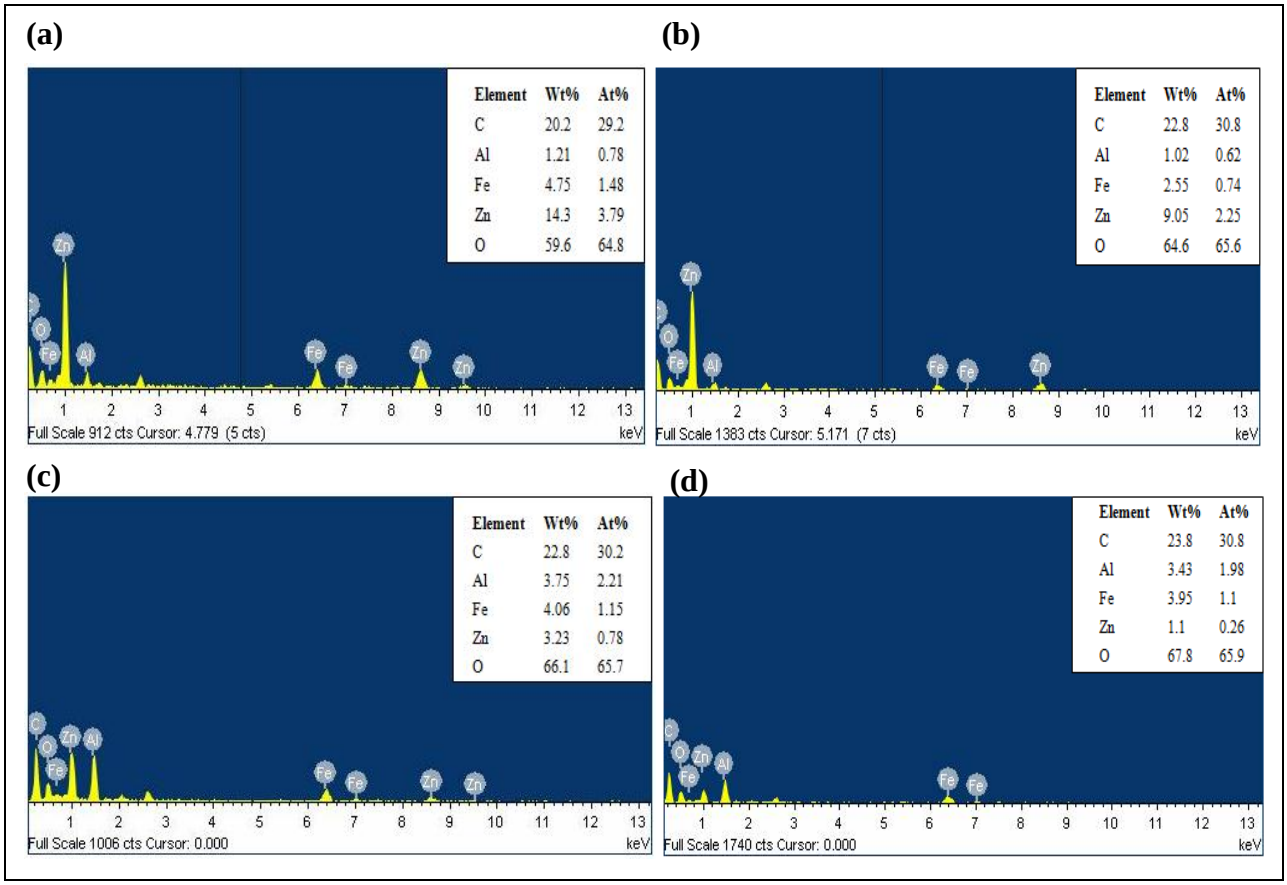

Figure 4.10: EDS analysis of laser cutting surface of A653 Galvanized steel sheet for (a) Exp. No. 21, (b) Exp. No. 6, (c) Exp. No. 4 and (d) Exp. No. 8.

EDS analysis shows the residuals of carbon, aluminium, iron, zinc and oxygen were presented in the laser machined sample. Figure 4.10 shows the weight % of oxygen and carbon are most as compared to others. The oxygen present in laser machined surface was due to oxidation as development of huge amount of temperature in the process. Oxygen reacts with other elements of material as results in evolution of compound like iron oxide, zinc oxide and

aluminium oxide. Iron oxide results in scaling. Formations of these compounds deteriorate the material properties like mechanical strength and surface topography.

4.2.5 Multi-objective Optimization

In the present work, three responses have been studied such as kerf width, kerf deviation and material removal rate. The main objective of present research to get the best optimum result, the value of kerf width and kerf deviation required to be minimum and value of MRR required being maximum. Nowadays, as competition increases single response optimization will not serve the purpose of industries because all responses have different nature and they contradict to each other. To overcome this problem multiple-objective optimization has emerged as one of the most successful tool which provides optimum result by simultaneous optimization of all responses by using developed models. The desirability function approach has been used for Multi-response optimization. Multiple responses combined and converted into single response called desirability function (d_i). The value of desirability function (d_i) ranges from 0 to 1. A zero represents that the one or more responses fall outside to their acceptance limit and one represents the ideal case [Kumar et al., 2013b]. As the value of d_i increases model becomes more desirable.

Table 4.5: Constraints of input and response parameters

Parameters	Goal	Lower Limit	Upper Limit	Lower Weight	Upper Weight	Importance
Gas Pressure		6	10	1	1	3
Power		80	100	1	1	3
Frequency		50	90	1	1	3
Feed		150	450	1	1	3
Kerf Width	minimize	0.241	0.489	1	1	3
Kerf deviation	minimize	0.238	0.416	1	1	3
MRR	maximize	218.75	802.17	1	1	3

Table 4.5 shows the upper and lower limit of input parameters and responses and also shows the goal, weights and importance assigned to each parameter. In Table 4.5 the value of lower and upper weight seems to be unity, it means all parameters are equally responsible for optimum result. RSM model computed twenty five optimized parametric solutions as shown in

Table 4.6. The best optimized solution satisfying above criteria has the overall desirability of 0.97. The optimal process parameter setting for minimum kerf width, kerf deviation and maximum material removal rate is gas pressure of 10 Kgf/cm^2, power 80 W, frequency 90 Hz and feed 198 mm/min.

Table 4.6: Combinations of Process parameters for high value of desirability

	Factors				Predicted responses			
Exp. No.	Gas Pressure	Power	Frequency	Feed	Kerf Width (mm)	Kerf deviation (mm)	MRR (mm/min)	Desirability
1	10	80	90	198	0.241	0.208	762	0.976
2	10	80	90	196	0.239	0.208	759	0.975
3	6	100	50	450	0.266	0.225	1058	0.965
4	10	80	89	190	0.241	0.220	738	0.962
5	6	100	50	450	0.269	0.228	1053	0.961
6	6	99	50	450	0.275	0.233	1030	0.953
7	6	100	51	444	0.279	0.237	1037	0.946
8	6	100	50	428	0.283	0.237	1031	0.940
9	10	83	90	175	0.241	0.223	672	0.919
10	10	80	90	450	0.327	0.157	942	0.867
11	10	80	90	323	0.328	0.206	887	0.865
12	10	80	90	450	0.328	0.158	942	0.865
13	10	80	90	450	0.332	0.160	940	0.859
14	6	94	50	450	0.303	0.266	869	0.858
15	10	80	89	309	0.340	0.219	802	0.843
16	8	100	50	450	0.333	0.249	877	0.839
17	10	100	90	450	0.345	0.200	805	0.835
18	10	100	90	446	0.354	0.203	782	0.807
19	9	100	89	450	0.357	0.205	782	0.801
20	10	100	90	403	0.354	0.222	747	0.790
21	9	100	50	450	0.328	0.275	772	0.788
22	9	100	90	449	0.364	0.206	761	0.777
23	10	92	90	450	0.382	0.209	857	0.755
24	10	100	90	276	0.318	0.252	532	0.698
25	10	96	90	274	0.348	0.263	598	0.682

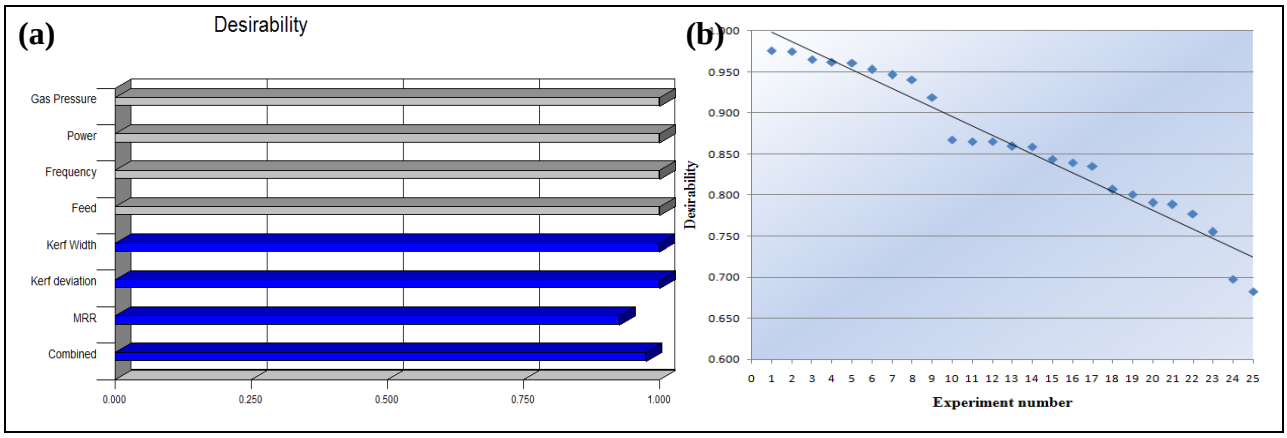

Fig. 4.11**:** (a) Desirability bar graph and (b) scatter plot between experiment number and desirability.

Figure 4.11 (a) shows the bar graph between different parameters and desirability function. It can observe that the kerf width and kerf deviation shows the value of desirability approximately equal to one. It was observed from the Fig. 4.11 (b) that as the experiment number increased the value of desirability decreased. Desirability value fall along the straight line which shows that value is normally distributed and model is feasible.

Confirmation test

Confirmation experiment was conducted to verify the improvement in performance characteristics. The confirmatory experiment was conducted to check the percentage of model prediction error between experimental result and predicted result by using Eq. (4.1).

$$\% \text{ Prediction error} = \frac{Experimental \quad result - Predicted \quad result}{Experimental \quad resu\,lt} \times 100 \qquad (4.1)$$

Table 4.7: Experimental validation of developed models at optimal parameter setting

Reponses	Experimental	Predicted	Error %
Kerf width (mm)	0.254	0.241	5.12
Kerf deviation (mm)	0.221	0.208	5.88
MRR (mg/min)	782	762	2.56

The percentage prediction error at optimal parameter setting is as shown in Table 4.7. The confirmation result shows the percentage prediction error in kerf width, kerf deviation and MRR are 5.12 %, 5.88 % and 2.56 % respectively. It is concluded that the experimental results are close to predicted results, hence it shows the predicted model is adequate and satisfactory.

4.3 Taguchi based Fuzzy logic

A hybrid approach of Taguchi based fuzzy logic was used for optimization of the multiple performance characteristics of laser cutting without considering interactions. The experiments were performed on 0.5 mm thick A653 Galvanized steel sheet using 100 W Fiber laser beam machine of continuous mode with Oxygen as assist gas. The S/N ratios obtained for all the quality characteristics are shown in Table 4.8.

Table 4.8: S/N ratios for different quality characteristics

Trail no	Gas Pressure (kgf/cm2)	Power (W)	Frequency (Hz)	Feed (mm/min)	SNR for KW	SNR for KD	SNR for MRR
1	6	80	50	150	8.947	10.487	40.294
2	6	80	70	300	9.465	7.597	50.486
3	6	80	90	450	8.914	6.196	56.625
4	6	90	50	300	8.636	12.505	57.001
5	6	90	70	450	8.535	12.111	56.478
6	6	90	90	150	11.13	11.903	46.533
7	6	100	50	450	9.396	9.422	56.89
8	6	100	70	150	10.653	10.145	52.839
9	8	100	90	300	9.87	6.411	55.693
10	8	80	50	300	8.031	5.288	57.421
11	8	80	70	450	9.053	9.119	60.928
12	8	80	90	150	11.277	10.089	50.95
13	8	90	50	450	8.699	8.09	56.586
14	8	90	70	150	9.499	9.119	40.599
15	8	90	90	300	8.223	8.589	52.085
16	8	100	50	150	9.603	7.013	43.522
17	8	100	70	300	7.908	5.832	59.184
18	8	100	90	450	8.581	8.826	56.586
19	10	80	50	450	8.81	9.473	57.947
20	10	80	70	150	10.712	7.766	42.477
21	10	80	90	300	10.015	6.09	45.46
22	10	90	50	150	7.487	5.368	48.755
23	10	90	70	300	8.922	7.453	49.005
24	10	90	90	450	8.722	6.994	57.501
25	10	100	50	300	8.201	5.482	50.344
26	10	100	70	450	8.201	10.903	49.629
27	10	100	90	150	11.491	12.111	43.522

The optimization procedure is given as:

i. Experiments were conducted using Taguchi's orthogonal array.
ii. Experimental results were converted into the signal-to-noise (S/N) ratio.
iii. Fuzzy model was developed by defining the input - output variables and fuzzy rules.
iv. A single FMRPI was computed by using fuzzy logic theory.
v. Experimental results were analyzed by using the FMRPI and analysis of variance (ANOVA).
vi. Optimum levels of process parameters were selected.

Fuzzy logic has emerged as one of the most successful tool for dealing with uncertain and vague information. In order to deal with such kind of problems fuzzy logic approach seems to be the most appropriate. Fuzzy logic approach provides decision support and expert system, with powerful reasoning mechanism, bound by sets of fuzzy IF-THEN rules used to drive conclusions from the given conditions. The fuzzy logic was modeled on Fuzzy logic toolbox of MATLAB v 7.11 (R2010b). The Mamdani fuzzy inference system was chosen due to its simplicity. The fuzzy model containing three input parameters (S/N ratios of KW, KD and MRR, respectively) and one output parameter (FMRPI) is shown in Fig. 4.12.

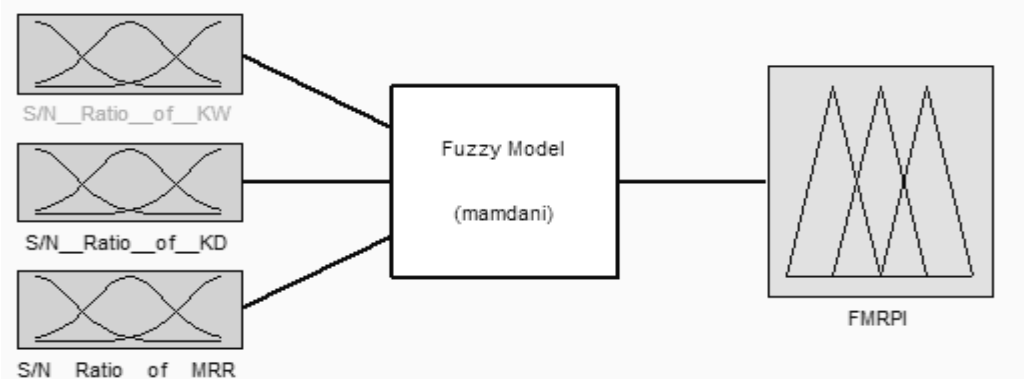

Figure 4.12: Input and output variables of the Fuzzy logic model

The input and output variables are defined as linguistic variables where their linguistic values are define in words or sentences. In the present work, three input variables having three linguistic values were defined namely, Small (S), Medium (M), High (H). Nine linguistic values were assigned to the output namely very very small (VVS), very small (VS), small (S), small

medium (MS), medium (M), medium high (MH), high (H), very high (VH) and very very high (VVH). Trapezoidal shape type membership functions were considered for input and output variables. The trapezoidal membership functions were applied for all input and output variables because trapezoidal shapes cover more range and are smooth as compare to Triangular shapes. The membership plots are shown in Fig. 4.13.

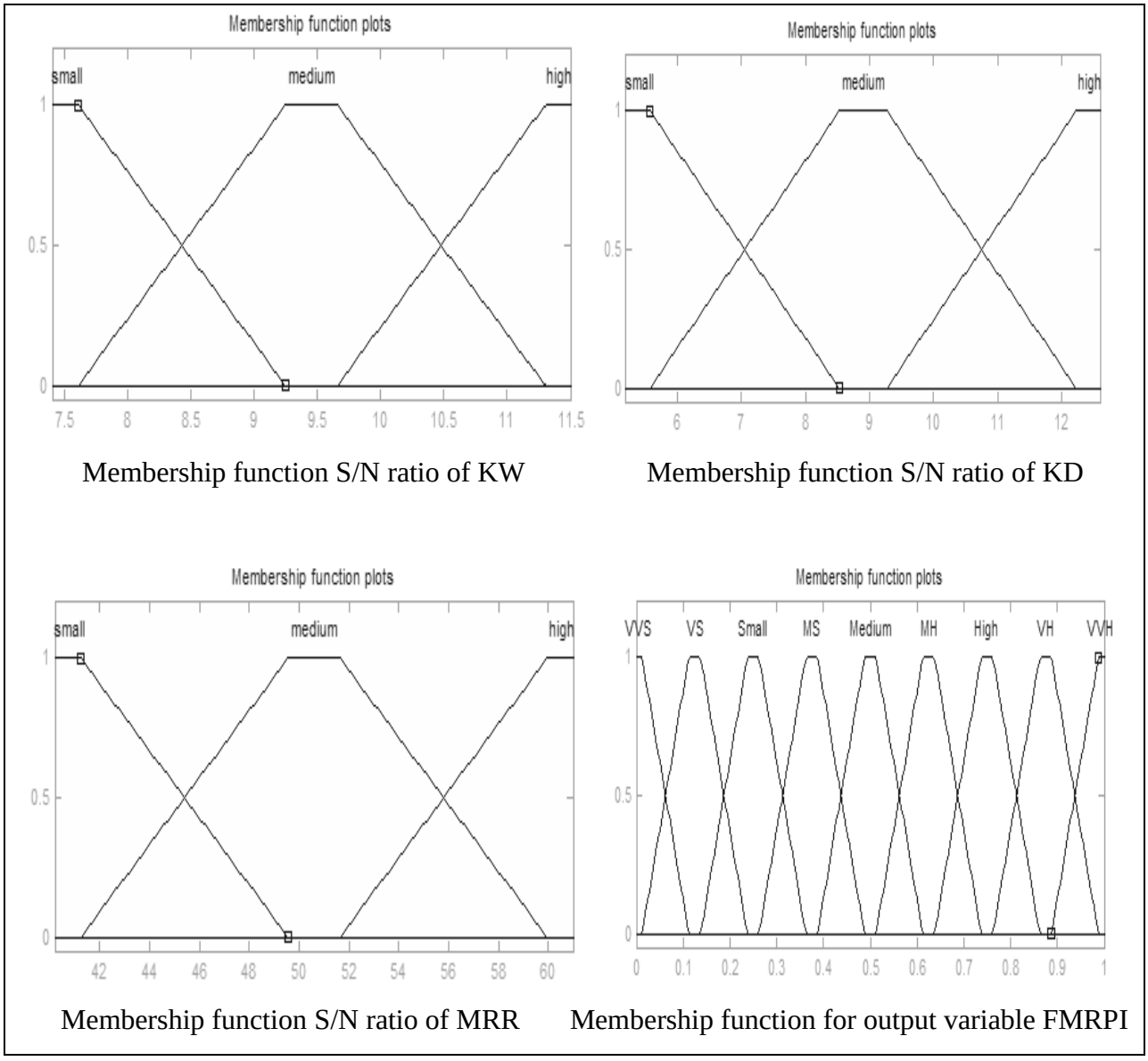

Membership function S/N ratio of KW

Membership function S/N ratio of KD

Membership function S/N ratio of MRR

Membership function for output variable FMRPI

4.13: Membership functions for input and output variables.

A total of twenty-seven fuzzy rules were developed for three input variables and their three linguistic values. A part of the rule viewer is shown in Fig. 4.14.

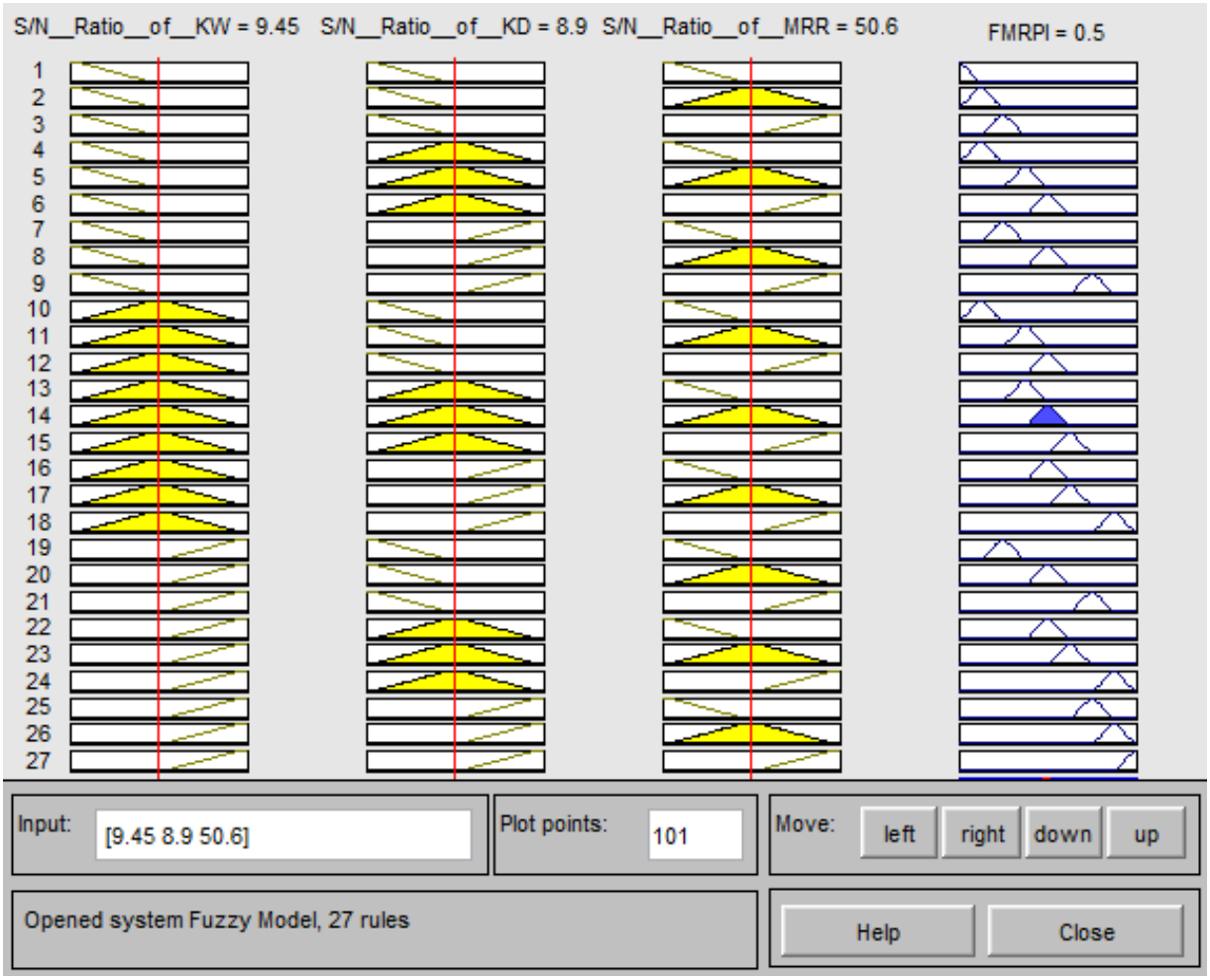

Figure 4.14: Rule viewer

4.3.1 Multi-objective Optimization using Fuzzy logic

The definition of performance characteristics such as lower-the-better, higher-the-better and nominal-the-better contains the degree of uncertainty and vagueness. So, fuzzy logic may be used to convert the S/N ratios of quality characteristics obtained by Taguchi into a fuzzy multi-response performance index (FMRPI). The FMRPI values obtained by Fuzzy model for each experimental run are shown in Table 4.9.

Table 4.9: Result of Fuzzy multi response performance index (FMRPI)

	Factors				
Trail no.	Gas pressure	Power	Frequency	Feed	FMRPI
1	6	80	50	150	0.362
2	6	80	70	300	0.457
3	6	80	90	450	0.406
4	6	90	50	300	0.715
5	6	90	70	450	0.695
6	6	90	90	150	0.748
7	6	100	50	450	0.597
8	6	100	70	150	0.664
9	6	100	90	300	0.536
10	8	80	50	300	0.29
11	8	80	70	450	0.607
12	8	80	90	150	0.705
13	8	90	50	450	0.461
14	8	90	70	150	0.375
15	8	90	90	300	0.435
16	8	100	50	150	0.295
17	8	100	70	300	0.32
18	8	100	90	450	0.515
19	10	80	50	450	0.573
20	10	80	70	150	0.385
21	10	80	90	300	0.324
22	10	90	50	150	0.123
23	10	90	70	300	0.379
24	10	90	90	450	0.411
25	10	100	50	300	0.225
26	10	100	70	450	0.493
27	10	100	90	150	0.77

Table 4.10 shows the mean FMRPI values of different levels of corresponding factors. The maximum average values of FMRPI were obtained at level 1 (6 kgf/cm^2) for gas pressure, level 3 (100 W) for power, level 3 (90 Hz) for frequency and level 3 (450 mm/min) for feed. Based on the response table and response graph, the optimal parameter settings for minimum kerf width, kerf deviation and maximum material removal rate is $A_1B_3C_3D_3$.

Table 4.10: Response table for FMRPI

Factor	Symbol	Unit	Fuzzy multi-response performance index		
			Level 1	Level 2	Level 3
Gas pressure	A	Kgf/cm^2	0.5756*	0.4448	0.4092
Power	B	KW	0.4566	0.4824	0.4906*
Frequency	C	Hz	0.4046	0.4861	0.5389*
Feed	D	mm/min	0.4919	0.409	0.5287*

Analysis of variance (ANOVA) is used to find the relative effect of different control factors and determine the most significant factors that affect the performance characteristics. Results of analysis of variance (ANOVA) are shown in Table 4.11. It was observed from the F and P values that the control factors A (Gas pressure), C (Frequency) and D (Feed) are significant. The F- value has been found at 95 % confidence level. Gas pressure is most significant factor with percentage contribution of 47.04 %.

Table 4.11: Results of ANOVA for multi-objective optimization

Factors	DOF	Seq SS	Adj SS	Adj SS	F-value	P-value	% Contribution
Gas pressure	2	0.1381	0.1381	0.0691	2.7	0.094	47.04
Power	2	0.0057	0.0057	0.0028	0.11	0.896	1.91
Frequency	2	0.0824	0.0824	0.0412	1.61	0.227	28.05
Feed	2	0.0676	0.0676	0.0338	1.32	0.292	23.01
Error	18	0.4607	0.4607	0.0256			
Total	26	0.7546					

4.3.2 Confirmation test

The confirmatory experiments were performed to predict and verify the improvement in performance characteristics. The predicted value of FMRPI, using optimal parameter level can be calculated by using Eq. (4.2).

$$\mu_{fmpi} = \mu_m + \sum_{i=1}^{n} (\mu_i - \mu_m) \quad (4.2)$$

Where μ_m is the total mean of FMRPI, μ_i is the mean of FMRPI at the optimal level and n is the number of control factors. Table 4.12 shows the comparison of predicted and experimental value at optimum level. Two experiments have been performed at predicted optimum level and average value of each quality characteristics obtained.

Table 4.12: Result of confirmation experiments for FMRPI

	Initial parameters settings	Optimal parameters setting	
		Predicted value	Experimental value
Setting level	A1B1C1D1	A1B3C3D3	A1B3C3D3
Kerf width (mm)	0.357		0.334
Kerf deviation (mm)	0.299		0.274
MRR (mm/min)	103.45		724
FMRPI	0.362	0.7043	0.719

The confirmation results show that the kerf width, kerf deviation and MRR were considerably improved. It was concluded that the kerf width and kerf deviation improved by reducing 6.44 % and 8.36 % respectively. The MRR value increased from 103.45 to 724 mm/min shows enormous improvement by 600 %. It was found that MRR increased due to increase in feed (from 150 to 450 mm/min) and power (from 80 to 100 W). This can be explained on the basis of increase in power density of beam cause more heat conduction and temperature rise and increase in feed rate cause more removal of material rate. The value of FMRPI corresponding to the confirmed experimental value was found as 0.719 and for predicted value it was found as 0.7043. The percentage prediction error for FMRPI obtained 2.04% that was almost negligible.

Chapter 5

Conclusion and Scope for Future work

5.1 Introduction

The present research work, investigate the effect of input parameters on quality characteristics such as kerf width, kerf deviation and MRR. The four input parameters gas pressure, power, frequency and feed have been selected to carry out the experimental study during fiber laser cutting of A653 Galvanized steel sheet.

5.1.1 Conclusion for Response surface methodology

Response surface methodology (RSM) technique was used to optimize the process parameters with considering the interactions. The effect of process parameters on each response is calculated by using mathematical model equation. From this work, the following conclusions could be drawn:

- Feed was identified as the most significant factor followed by gas pressure, frequency and power for kerf width, kerf deviation and MRR.
- The value of MRR increased from 275 to 676 mm/min as gas pressure 6 to 10 kgf/cm^2 and feed increased from 150 to 450 mm/min, it revealed that the interaction between gas pressure and feed has most significant effect on MRR. Interaction between frequency and feed has significant effect on kerf width.
- The developed mathematical models for kerf width, kerf deviation and MRR are adequate. These models successfully proposed for direct evaluation of kerf width, kerf deviation and MRR for different parametric setting during fiber laser cutting of A653 Galvanized steel sheet.
- Normal plot of residuals are along the straight line and points are close to each other implying that the error terms are normally distributed.

- For multi-objective optimization the optimal parameters setting for minimum kerf width, kerf deviation and maximum material removal rate is gas pressure of 10 Kgf/cm^2, power 80 W, frequency 90 Hz and feed 198 mm/min.
- The optimum results value verified by confirmatory experiments shows the percentage prediction error for kerf width 5.12 %, kerf deviation 5.88 % and MRR 2.56 % respectively. This is almost negligible. Hence, it is concluded that RSM is suitable for prediction of fiber laser cutting process.

5.1.2 Conclusion for Taguchi based Fuzzy logic

The Taguchi based Fuzzy logic theory was used to optimize multiple responses KW, KD and MRR in laser cutting process assuming no interaction between the input factors. The following conclusions of the paper are given below:

- Taguchi method with fuzzy logic approach easily employed to optimize multiple responses in laser cutting process. This approach is more flexible and superior to other optimization techniques.
- The experimental results for optimal settings showed that the geometrical accuracy of laser cut was considerably improved by reducing the kerf width, kerf deviation by 6.44% and 8.36% and increasing the material removal rate (MRR) enormously.
- The experimental results indicate that the oxygen gas pressure was the most significant factor followed by frequency and feed. The percentage contribution of oxygen gas pressure, frequency and feed for multi-objective optimization were found as 47%, 28% and 23% respectively.
- The predicted optimum results value verified by confirmation experiments shows that the percentage prediction error of 2.04 % that is almost negligible. Hence it is concluded that the present fuzzy expert model is suitable for prediction Fiber laser cutting process with negligible error.

5.1.3 Conclusion for Surface topography analysis

- It was observed that HAZ value decreases (from 1.2 to 0.52 mm) with increase in gas pressure (from 6 to 10 Kgf/cm^2) and increase in feed (from 150 to 450 mm/min). Due to the contact time between work material and laser beam shortened greatly, which results in less HAZ. HAZ value increased from 0.520 to 1.35 mm with increase in power and frequency. Power and frequency have significant effect on HAZ. This can be explained by as the power and frequency increases, the intensity of laser beam increases excessive amount of heat produced and increases the HAZ
- It was concluded from the SEM analysis that during laser cutting process excessive heat and melting or vaporizing of work material caused the formation of deep, overlapping craters and molten material is deposited in the form of globules of debris. The formation of recast layer and craters also observed during laser beam machining that could be due to uneven distribution of laser beam energy.
- The formation of recast layer decreases as gas pressure increases from 6 kgf/cm^2 to 10 kgf/cm^2. This is due to as gas pressure increases more molten material blows away from the cutting zone so very less material left to resolidified to form recast layer. Gas pressure is most significant factor which effect on recast layer.
- The residuals of carbon, aluminium, iron, zinc and oxygen were detected in laser machined samples using EDS analysis. Presence of oxygen occurs due to oxidation. From the analysis it was found that different compounds formed like aluminium oxide, zinc oxide and iron oxide.

5.2 Scope for Future work

- Most of the literature reviewed related to laser cutting followed by drilling and micromachining. There is a large scope of research in the area of 3-D LBM like turning and milling which is still awaiting in industry. [Dubey and Yadava, 2008a].
- There is a large scope of research by using some other undesired factors which affect the performance variations such as (assist gas type, beam spot diameter, thermal conductivity and reflectivity of workpiece, focal distance, standoff distance) still need to be considered to increase the surface quality.

- Most of the literature available in this area has concentrated on a single quality characteristic. Optimum value of process parameters for one quality characteristic may affect the overall quality. There is a large scope available on multi-objective optimization of LBM process.
- Very few researchers consider the effect of interaction parameters on laser beam machining process. There is large scope to investigate the interaction parameters effect on laser beam machining process.
- Most of the researchers consider straight cutting profile of workpiece. There is vast scope to study the other geometric profile like circular, curved and zigzag and find the effect of process parameters on quality characteristics of laser beam machined surface.

References

Chang, C.W.; Kuo, C.P. (2007) Evaluation of surface roughness in laser-assisted machining of aluminium oxide ceramics with Taguchi method.*International Journal of Machine Tools & Manufacture*, 47: 141–147.

Dubey, A.K.; Yadava, V. (2008a) Laser beam machining-A review.*International Journal of Machine Tools & Manufacture*, 48:609–628.

Dubey, A.K.; Yadava, V. (2008b) Multi-objective optimisation of laser beam cutting process.*Journal of Optics and Laser Technology*, 40:562-570.

Dubey, A.K.; Yadava, V. (2008c) Optimization of kerf quality during pulsed laser cutting of aluminium alloy sheet.*Journal of materials processing technology*, 204:412-418.

Dewangan, S.; Gangopadhyay, S.; Biswas, C.K. (2015) Study of surface integrity and dimensional accuracy in EDM using Fuzzy TOPSIS and sensitivity analysis.*Measurement*, 63:364-376.

Ghosal, A.; Manna, A. (2013) Response surface method based optimization of ytterbium fiber laser parameter during machining of Al/Al2O3-MMC.*Optics & laser technology*, 46:67-76.

Jeyapaul, R.; Jenarthanam, M.P. (2013) Analysis and optimisation of machinability behavior of GFRP composites using Fuzzy logic.*International conference on Sustainable manufacturing and operations management*, 121-128.

Kumar, A.; Kumar, V.; Kumar, J. (2013a) Investigation of machining parameters and surface integrity in wire electric discharge machining of pure titanium.*Journal of Engineering Manufacture*, 227-7:972-992.

Kumar, A.; Kumar, V.; Kumar, J. (2013b) Surface integrity and material transfer investigation of pure titanium for rough cut surface after wire electro discharge machining.*Journal of Engineering Manufacture*, 20-10:1-22.

Madic, M.; Radovanovic, M.; Nedic, B. (2012) Correlation between surface roughness characteristics in CO_2 laser Cutting of mild steel.*Journal of Tribology in Industry*, 34-4:232-238.

Madic, M.; Radovanovic, M.; Slatineanu, L. (2013) Surface roughness optimization in CO_2 laser Cutting by using taguchi method.*U.P.B. Sci. Bull* 75-1:97-106.

Pandey, A.K.; Dubey, A.K. (2011) Intelligent modeling of Laser cutting of thin sheet.*International Journal of Modeling and Optimization,* 1-2:107-112.

Pandey, A.K.; Dubey, A.K. (2012) Taguchi based fuzzy logic optimization of multiple quality characteristics in laser cutting of Duralumin sheet.*Journal of Optics and Laser in Engineering,* 50:328-335.

Pandey, A.K.; Dubey, A.K. (2013) Fuzzy expert system for prediction of kerf qualities in pulsed laser cutting of Titanium alloy sheet.*International Journal of Machining Science and Technology,* 17-4:545-574.

Pawar, P.J.; Rayate, G.B. (2014) Multi-objective Optimization of Laser Beam Machining Process Parameters.*International Journal of Advanced Mechanical Engineering,* 4:257-262.

Phipon, R.; Pradhan, B.B. (2012) Control parameters optimization of Laser beam machining using Genetic algorithm.*International Journal of Computational Engineering Research,* 1-5:1510-1516.

Shabgard, M.R.; Badamchizadeh, M.A.; Ranjbary, G.; Amini, K. (2013) Fuzzy approach to select machining parameters in electrical discharge machining (EDM) and ultrasonic-assisted EDM processes.*Journal of Manufacturing systems,* 32:32-39.

Shah, V.K.; Patel, H.J.; Patel, D.M. (2014) Optimization of input parameters on surface roughness during laser cutting -a review.*International Journal For Technological Research In Engineering,* 1-5: 238-240.

Sharma, A.; Yadava, V. (2012) Modelling and optimization of cut quality during pulsed Nd:YAG laser cutting of thin Al-alloy sheet for straight profile.*Optics & laser technology* 44:159-168.

Sivarao.; Brevern, P.; El-Tayeb, N.S.M. (2009) A new approach of Adaptive Network-based fuzzy inference system modeling in laser processing-a graphical user interface based.*Journal of Computer Science,* 5-10:704-710.

Syn, C.Z.; Mokhtar, M.; Feng, C.J.; Manurung, Y.H.P. (2011) Approach to prediction of laser cutting quality by employing fuzzy expert system.*Journal of Expert Systems with Applications,* 38:7558-7568.

Bai, Y.; Wang, D. (2006) Fundamentals of Fuzzy Logic Control – Fuzzy Sets, Fuzzy Rules and Defuzzifications.Advanced Fuzzy Logic Technologies in Industrial Applications (http://www.springer.com/978-1-84628-468-7)

Majumdar, J.D.; Manna, I. (2013) Introduction to Laser-Assisted Fabrication of Materials. *Springer Series in Materials Science,* 161:668-735. (http://www.springer.com/978-3-642-28358-1)

Balasubramaniam, R. (2014) Callister's Material Science and Engineering.*Wiley India Pvt. Ltd.*

Ghosh, A.; Mallik, A.K. (2010) Manufacturing Science. *Affiliated East–West Press*, 1985

Rajasekaran, S.; Pai, G.A.V. (2010) Neural Networks, Fuzzy Logic, and Genetic Algorithms. *PHI Learning Private Limited*

Rao, R.V. (2011) Advanced modeling and optimization of manufacturing processes.*Springer-Verlag London Limited*

Web References:

W.1 Laser beam machining, http://www.nptel.ac.in/courses/112105127/pdf/LM-40.pdf, (accessed on – 04/11/2014).

W.2 Galvaco Industries, http://www.galvaco.com/13143.html, (accessed on – 08/03/2015)